NAVAL POSTGRADUATE SCHOOL
MONTEREY, CALIFORNIA

THESIS

THEORETICAL AND EXPERIMENTAL INVESTIGATION OF THE RESPONSE OF A ROTOR ACCELERATING THROUGH CRITICAL SPEED

b y

Gregory L. Reed

December, 1995

Thesis Advisor: Knox T. Millsaps, Jr.

Approved for public release; distribution is unlimited.

REPORT DOCUMENTATION PAGE

Form Approved OMB No. 0704-0188

1. AGENCY USE ONLY *(Leave blank)*	2. REPORT DATE	3. REPORT TYPE AND DATES COVERED
	December 1995	Master's Thesis

4. TITLE AND SUBTITLE THEORETICAL AND EXPERIMENTAL INVESTIGATION OF THE RESPONSE OF A ROTOR ACCELERATING THROUGH CRITICAL SPEED.

5. FUNDING NUMBERS

6. AUTHOR(S) Gregory L. Reed

7. PERFORMING ORGANIZATION NAME(S) AND ADDRESS(ES)
Naval Postgraduate School
Monterey CA 93943-5000

8. PERFORMING ORGANIZATION REPORT NUMBER

9. SPONSORING/MONITORING AGENCY NAME(S) AND ADDRESS(ES)

10. SPONSORING/MONITORING AGENCY REPORT NUMBER

11. SUPPLEMENTARY NOTES The views expressed in this thesis are those of the author and do not reflect the official policy or position of the Department of Defense or the U.S. Government.

12a. DISTRIBUTION/AVAILABILITY STATEMENT
Approved for public release; distribution is unlimited.

12b. DISTRIBUTION CODE

13. ABSTRACT *(maximum 200 words)*

The rotordynamic response of an imbalanced rotor accelerating through its first lateral bending critical speed was investigated both analytically and experimentally. A two degree-of-freedom lumped mass, damping and stiffness model was developed to simulate the response of a simply supported, single disk rotor during both acceleration and deceleration. The equations of motion were then solved numerically. The computer model was used to determine the effect of acceleration rate, asymmetric stiffness and damping, and acceleration scheduling on the maximum amplitude of the response. Experimental data for a simply supported, single disk rotor accelerating at different rates were compared with the computer model. Increased acceleration rates and damping reduce the magnitude of the response. Asymmetric stiffness and acceleration scheduling can also be used advantageously to reduce the maximum amplitude of the response.

14. SUBJECT TERMS Accelerating Rotor			15. NUMBER OF PAGES 69
			16. PRICE CODE
17. SECURITY CLASSIFICATION OF REPORT Unclassified	18. SECURITY CLASSIFICATION OF THIS PAGE Unclassified	19. SECURITY CLASSIFICATION OF ABSTRACT Unclassified	20. LIMITATION OF ABSTRACT UL

NSN 7540-01-280-5500

Standard Form 298 (Rev. 2-89)
Prescribed by ANSI Std. 239-18 298-102

Approved for public release; distribution is unlimited.

THEORETICAL AND EXPERIMENTAL INVESTIGATION OF THE RESPONSE OF A ROTOR ACCELERATING THROUGH CRITICAL SPEED

Gregory L. Reed
Lieutenant, United States Navy
B.S., Purdue University, 1986

Submitted in partial fulfillment
of the requirements for the degree of

MASTER OF SCIENCE IN MECHANICAL ENGINEERING

from the

NAVAL POSTGRADUATE SCHOOL
December 1995

Author: 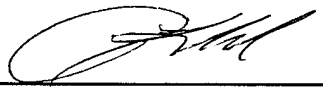

Gregory L. Reed

Approved by: 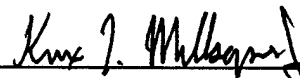

Knox T. Millsaps, Jr., Thesis Advisor

Matthew D. Kelleher, Chairman
Department of Mechanical Engineering

ABSTRACT

The rotordynamic response of an imbalanced rotor accelerating through its first lateral bending critical speed was investigated both analytically and experimentally. A two degree-of-freedom lumped mass, damping and stiffness model was developed to simulate the response of a simply supported, single disk rotor during both acceleration and deceleration. The equations of motion were then solved numerically. The computer model was used to determine the effect of acceleration rate, asymmetric stiffness and damping, and acceleration scheduling on the maximum amplitude of the response. Experimental data for a simply supported, single disk rotor accelerating at different rates were compared with the computer model. Increased acceleration rates and damping reduce the magnitude of the response. Asymmetric stiffness and acceleration scheduling can also be used advantageously to reduce the maximum amplitude of the response.

TABLE OF CONTENTS

LIST OF SYMBOLS

SYMBOL	DEFINITION (units, U.S. Customary)
M	Mass of the system. (lbm)
m	Mass of the imbalance. (lbm)
e	Distance from shaft centerline to center of mass imbalance. (in)
F	Force. (lbf)
θ	Angle. (radians)
K_{xx}	x direction stiffness caused by x direction displacement. (lbf/in)
K_{yy}	y direction stiffness caused by y direction displacement. (lbf/in)
K_{xy}	x direction stiffness caused by y direction displacement. (lbf/in)
K_{yx}	y direction stiffness caused by x direction displacement. (lbf/in)
C_{xx}	x direction damping caused by x direction velocity. (lbf-sec/in)
C_{yy}	y direction damping caused by y direction velocity. (lbf-sec/in)
C_{xy}	x direction damping caused by y direction velocity. (lbf-sec/in)
C_{yx}	y direction damping caused by x direction velocity. (lbf-sec/in)
P	Magnitude of the forcing function. (lbf)
h	Acceleration of the system. (cycles/sec^2)

σ	Initial phase angle of the exciting force. (radians)
t	Time. (seconds)
r	Number of undamped free vibrations from time zero to time t. (cycles)
q	Value of r at which the instantaneous frequency of the exciting force is equal to the natural frequency of the system. (non-dimensional)
ω	Instantaneous frequency of the exciting force. (radians/second)
ω_n	Natural frequency of the system. (radians/second)
N	Natural frequency of the system. (cycles/second)
ζ	Damping ratio. (non-dimensional)

I. INTRODUCTION

Rotating machinery is used widely throughout the world in numerous applications. These applications include gas and steam turbines for propulsion and electrical power generation, power transmission shafting, compressors, pumps, gyroscopes, high speed flywheels, and several other devices used in all disciplines and areas of engineering.

Many of these rotating machines are normally operated above their first or second critical speeds and therefore must pass through one or more critical speeds when being started and again when coming to rest. Therefore, the problem of determining the maximum amplitudes and stresses in the system due to the forced vibrations during acceleration through critical speed is of vital interest. Of even greater interest is the determination of what methods could be used to reduce the maximum amplitudes of the lateral bending response as these rotors pass through their critical speeds. This is especially important in applications such as modern turbomachinery where the clearances between the rotor and the housing are becoming increasingly tight. The current trend toward higher spin rates to raise the power density and tighter clearances to increase the operating efficiency aggravates the problem of lateral vibration further. As the demand for high technology rotor systems increases, so does the need for the ability to accurately predict and analyze the dynamic response. The proper prediction and understanding of the machine dynamics, especially during the design phase, will allow for the use of lighter materials, higher obtainable speeds, and more power dense machines while decreasing maintenance or even catastrophic failure.

Rotating machinery can experience several modes of vibration. The lateral vibrations are of primary concern here. Due primarily to residual imbalance in the rotating members, lateral vibrations are the most common type encountered. Lateral vibrations

bring the possibility of rubbing or equipment damage due to the close tolerances of turbomachinery. In addition, the alternating stresses generated by these vibrations can damage bearings, and non-synchronous whirling can lead to fatigue of the rotor shafting.

The phenomena associated with rotating shafts which need to be studied and fully understood include; the response at or transitioning through critical speeds, shaft whirl, oil whip, chatter, bearing effects, and mounting effects.

The objectives of this research were to investigate how the different physical parameters such as rate of acceleration, stiffness and damping asymmetry, and the effect of acceleration scheduling effect the maximum amplitude of the response as a rotor is accelerated through its first lateral bending critical speed. In addition, to further develop the rotordynamic laboratory at the Naval Postgraduate School to facilitate the study of an accelerating rotor, including the creation of a mounting table for isolation of the rotor and to permit mounting of the rotor kit in any one of three orientations with respect to gravity.

In Chapter II a brief background of the pertinent literature on non-constant frequency excitation to support the research is provided.

In Chapter III a two degree-of-freedom analytical model is developed in which the ability to vary the rate of acceleration, amount of imbalance, stiffness and damping terms, and initial and final rpms is provided. The physical characteristics of the model are discussed and the equations of motion are provided along with the method of solution. The results of the model are compared to both the model of Lewis [Ref. 1] which is for a single degree-of-freedom and to the steady state Vejvoda [Ref. 2] model given an extremely slow rate of acceleration. Parameters are varied to examine how each effects the amplitude of the response in the model and an interpretation of the results is provided.

An explanation of all upgrades, changes, and additions to the experimental facility is provided in Chapter IV along with experimental results which are compared to the numerical model.

Chapter V contains a discussion of the results from both the numerical models and the experiments.

Finally, conclusions and recommendations are provided in Chapter VI.

II. BACKGROUND

A. HISTORICAL PERSPECTIVE

The first documented work on the dynamics of rotating shafts was presented by Rankine [Ref. 3] in 1869. His analysis dealt with the steady state response of rotors. Neglecting Coriolis acceleration, Rankine came to the mistaken conclusion that supercritical operation, that is, operating at an angular velocity greater than one or more of the systems natural frequencies, was statically unstable and therefore not possible for rotating machinery.

In 1919, Jeffcott [Ref. 4] published what has become one of the definitive references on the dynamics of rotating shafts. Analyzing the effects of imbalance on the steady state response of a rotating shaft, Jeffcott corrected the mistake made by Rankine, showing that supercritical operation was not only possible but could be beneficial. Obtaining the supercritical condition, however, required transitioning through the first critical speed where the frequency of the forcing function was equal to the first lateral bending natural frequency of the system and where large amplitude vibrations occurred. The Jeffcott rotor was developed, which is comprised of a long shaft with a concentrated mass disk and provides one of the simplest and most accurate models with which to study a simply supported rotating shaft.

The first analysis which dealt with a system accelerating through its critical speed was published in 1932 by Lewis [Ref. 1]. Lewis found the exact analytical solution of a linearly damped, single degree-of-freedom system accelerated uniformly from rest through its critical speed in terms of Fresnel's integrals. The figure he generated for the case of zero damping is still frequently reproduced. Lewis verified analytically that there is a decrease in the amplitude of the deflection and an apparent shift in the critical speed of a

system which accompanies an increase in the rate of acceleration. This is a shift to the right, or a higher apparent critical speed, for acceleration and a shift to the left for deceleration. Lewis also attempted to provide empirical formulas for the amount of reduction in amplitude and the amount of shift given large values of acceleration. Although his model was not one of a rotating reference frame, qualitatively his findings are still approximately valid for a rotating shaft experiencing acceleration through its critical speed. The Lewis results are used widely as rotors are normally accelerated through their critical speeds as quickly as possible.

Study in the area of acceleration through critical speeds continued. In 1939, Baker [Ref. 5] published his results on the Mathematical-Machine determination of the vibrations of an accelerated, unbalanced rotor.

In 1947, Meuser and Weibel [Ref. 6] presented a generalized solution for the response of a single degree-of-freedom system having linear plus cubic elasticity, and linear or viscous damping accelerating through its critical speed.

In 1949, McCann and Bennett [Ref. 7] extended the Lewis model to a two degree-of-freedom model and obtained solutions on an "electric-analog computer."

In 1966, by introducing asymptotic expressions for the Fresnel integrals, Fearn and Millsaps [Ref. 8] derived simple algebraic expressions which give values for the maximum amplitude and the frequency of the driving force where the maximum displacement occurs in the Lewis model.

Gluse [Ref. 9] in 1967, investigated the case of a rotor being accelerated through its critical speed by a constant applied torque rather than a constant angular acceleration. His analysis centered on the case of an unsuccessful acceleration, that is, an acceleration to the vicinity of critical speed but not through to the supercritical area. This is caused by the inertia forces which produce large lateral deflections which develop counter torques opposing the driving torque in the vicinity of the system natural frequency. Gluse

concluded that failure to accelerate through critical speed resulted from either insufficient driving torque or excessive imbalance of the rotor.

In 1992, Ishida, Yamamoto, and Murakami [Ref. 10] investigated analytically the non-stationary vibration characteristics during acceleration through a critical speed of a 1/3-order sub-harmonic oscillation of forward precession of a rotating shaft system. They concluded that the maximum amplitude during acceleration depends upon the angular acceleration rate, the initial disturbance (if one exists), the initial angular velocity, and the initial angular position of the imbalance.

In 1988, Vance [Ref. 11] analyzed the phenomena caused by bearing stiffness asymmetry in an imbalanced rotor. His observations included the phenomena of a split resonance peak in the response caused by this asymmetry and the resultant backward whirl when the rotational speed is between these two frequencies.

In 1994, Vejvoda [Ref. 2] developed a two degree-of-freedom, steady state analytical model and utilized an experimental rotor facility to investigate the cause of split-resonance and backward whirl phenomena. Isolating the effects of geometric imperfections in the bearing sleeves, gravitational forces, and bearing support stiffnesses, Vejvoda concluded that the stiffness asymmetry is responsible for the split resonance and backward whirl observed in his experiments. He also noted that the rotor system orientation with respect to the gravitational force and the mount isolation caused the rotor response to change.

III. ANALYTICAL MODEL

A. MODEL DEVELOPMENT

In order to predict the rotordynamic response of a rotor accelerating through it's critical speed, an analytical model was developed. The rotor was modeled as a two degree-of-freedom (x and y), lumped mass and lumped stiffness shaft and disk assembly as shown in Figure 1. The stiffnesses and cross-stiffnesses of the shaft, bearings, and support structures have been combined into single K_{XX}, K_{yy}, K_{Xy} and K_{yX} terms. Similarly, the proportional damping of the entire system has been combined into single C_{XX}, C_{yy}, C_{Xy}, and C_{yX} terms. By concentrating all of the systems properties into a single axial plane, this model provides a simple way to parametrically study the effects of direct and cross-coupled linear stiffness and damping on the maximum response amplitudes of an accelerating rotor. The model is limited in that no variations in the axial direction are taken into account, only forces which are linearly related to the displacements and velocities of the rotor are included, and in that the two bearings and their supports of the simply supported shaft are treated as identical, but not necessarily symmetrical in the x and y directions. Unlike the model in [Ref. 2] in which only the steady state response was of interest, an acceleration term has been added to permit the investigation of rotor response during acceleration and deceleration.

The equations of motion for this model system are as follows:

$$M\ddot{x} + C_{xx}\dot{x} + C_{xy}\dot{y} + K_{xx}x + K_{xy}y = me(\ddot{\theta}\cos\theta - \dot{\theta}^2\sin\theta) \quad (1)$$

$$M\ddot{y} + C_{yy}\dot{y} + C_{yx}\dot{x} + K_{yy}y + K_{yx}x = me(\ddot{\theta}\sin\theta + \dot{\theta}^2\cos\theta) \quad (2)$$

Where M is the total modal mass of the system modeled as a pinned-pinned beam as in [Ref. 2], m is the mass of the imbalance, e is the distance from the center of the shaft to the center of the mass imbalance and $\ddot{\theta}$ is constant. In the steady state case, the angular acceleration term $\ddot{\theta}$ goes to zero and magnitude of the forcing function is dependent only on the amount of imbalance and the rotor speed.

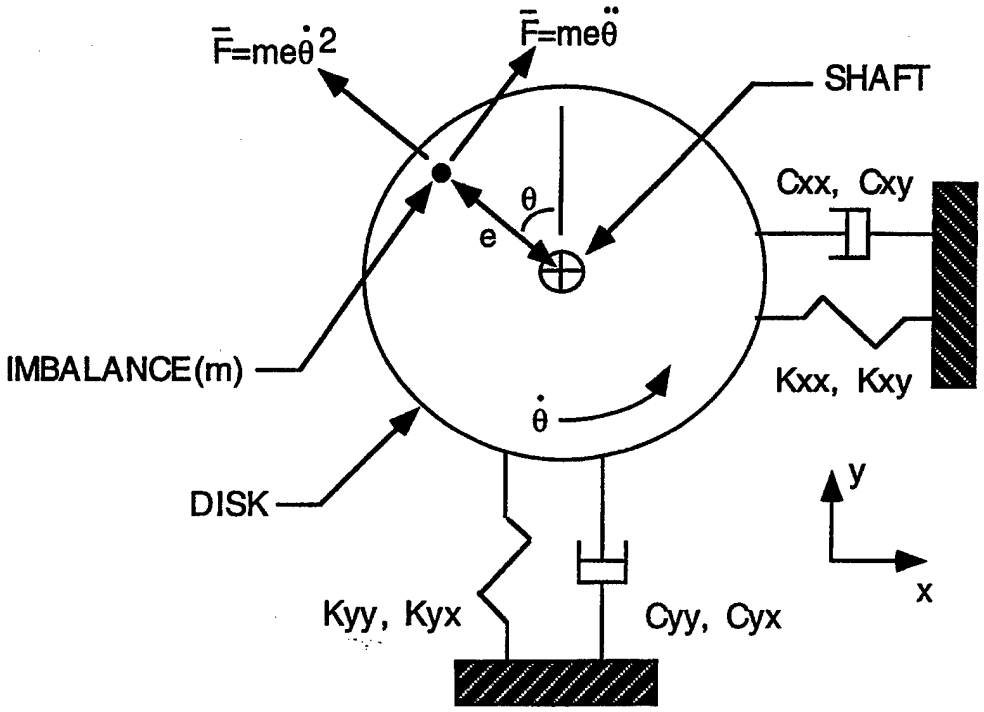

Figure 1. Two Degree-of-Freedom Lumped Mass and Stiffness Model of Rotating Shaft and Disk Assembly with Direct and Cross-Coupled Linear Stiffness and Damping.

Equations (1) and (2) can also be written in matrix form as:

$$\begin{bmatrix} M & 0 \\ 0 & M \end{bmatrix}\begin{Bmatrix} \ddot{x} \\ \ddot{y} \end{Bmatrix} + \begin{bmatrix} Cxx & Cxy \\ Cyx & Cyy \end{bmatrix}\begin{Bmatrix} \dot{x} \\ \dot{y} \end{Bmatrix} + \begin{bmatrix} Kxx & Kxy \\ Kyx & Kyy \end{bmatrix}\begin{Bmatrix} x \\ y \end{Bmatrix} = me\begin{Bmatrix} \ddot{\theta}\cos\theta - \dot{\theta}^2\sin\theta \\ \ddot{\theta}\sin\theta + \dot{\theta}^2\cos\theta \end{Bmatrix} \tag{3}$$

B. SOLUTION TECHNIQUE

These equations can be numerically solved using the Runge-Kutta method. For this method to be used, the two second-order differential equations (1) and (2) can be written as the following four first-order equations:

$$\dot{x}_2 = \left(\frac{me}{M}\right)\left(\ddot{\theta}\cos\theta - \dot{\theta}^2\sin\theta\right) - \left(\frac{Cxx}{M}\right)x_2 - \left(\frac{Cxy}{M}\right)y_2 - \left(\frac{Kxx}{M}\right)x_1 - \left(\frac{Kxy}{M}\right)y_1 \tag{4}$$

$$\dot{x}_1 = x_2 \tag{5}$$

$$\dot{y}_2 = \left(\frac{me}{M}\right)\left(\ddot{\theta}\sin\theta + \dot{\theta}^2\cos\theta\right) - \left(\frac{Cyy}{M}\right)y_2 - \left(\frac{Cyx}{M}\right)x_2 - \left(\frac{Kyy}{M}\right)y_1 - \left(\frac{Kyx}{M}\right)x_1 \tag{6}$$

$$\dot{y}_1 = y_2 \tag{7}$$

Several computer programs were written in MATLAB to solve these equations with the ability to enter the mass imbalance, Kxx, Kyy, Kxy, Kyx, Cxx, Cyy, Cxy, Cyx, initial and final shaft RPM, and the rate of acceleration as variables. The programs utilized the MATLAB function ODE45 which uses the fourth and fifth order Runge-Kutta methods. The initial conditions for this numerical method were determined by the analytic solution of the steady state (constant speed) response for the initial speed selected. θ(t=0) equal to zero was used but could be changed in the code.

Since the ODE45 program selects it's own time divisions for the numerical integration, the program did not allow for the interactive entry of acceleration as a function of time but only as a constant. However, acceleration as a function of time can be used if

entered directly in the code of the MATLAB function used in the ODE45 program. This function contains the 1st order differential equations of motion (equations (4) through (7)) and is called runga.m for the acceleration program. In addition, a program was written which allowed the rate of acceleration to be instantaneously changed at a given RPM. This allowed for the limited study of acceleration scheduling which will be discussed further at the end of this chapter.

C. MODEL VALIDATION

In order to validate the output of the computer models, two comparisons were made with the model results:

Lewis [Ref. 1] determined the exact solution to the problem of transitioning a system having a single degree of freedom and linear damping through its critical speed from rest at a uniform acceleration. The plot of his results using zero damping are often reproduced. The Lewis model used a forcing function of increasing frequency but with a constant amplitude:

$$f(t) = P \cos (\pi h t^2 + \sigma) \qquad (8)$$

where P is the magnitude of the forcing function, h is the acceleration of the system in cycles per second per second and σ is the initial phase angle of the exciting force.

The forcing function of an accelerating imbalanced rotor is not only one of increasing frequency but of increasing amplitude as well. Therefore, to compare the model with Lewis' results, it was changed to a two degree of freedom system with forcing functions in the x and y directions which were 90 degrees out of phase and were of a constant amplitude.

A plot of the results showing the maximum response curves for various values of q is shown in Figure 2 in the non-dimensionalized terms used by Lewis. The term r is the

number of undamped free vibrations the system would make from time zero to time t. The non-dimensionalized acceleration rate q, is given by:

$$q = N^2/h \tag{9}$$

where N is the natural frequency of the system in cycles per second and h is the acceleration in cycles per second per second. The term q can also be stated as the value of r at which the instantaneous frequency of the exciting force is equal to the natural frequency of the system. The amplitude term R, is given by:

$$R = Kx/P \tag{10}$$

where x is the displacement, k is the system stiffness and P is the magnitude of the forcing function. The results obtained by the model match very closely with the analytical solution presented by Lewis.

The next comparison made was with the steady state or constant excitation frequency analytical model of Vejvoda [Ref. 2]. Since the ODE45 program integrates from an initial time to a final time, zero acceleration could not be entered into the numerical program. However, an extremely slow acceleration should fall very closely to the results of the Vejvoda model. Figure 3 shows the amplitude -vs- rpm plots of both the analytical steady state response using the Vejvoda model and the numerical model response with an acceleration of 1 rpm/sec. This plot shows that the numerical model with a very slow rate of acceleration does, in fact, very nearly collapse to the results of the steady state analytical model.

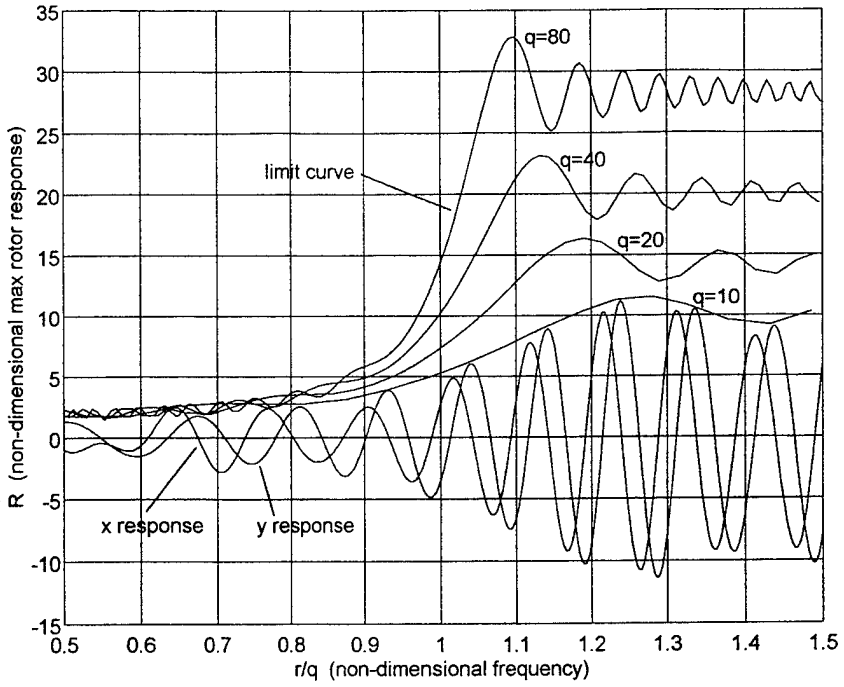

Figure 2. Model Results Using the Lewis Non-Dimensionalized Terms with Zero Damping.

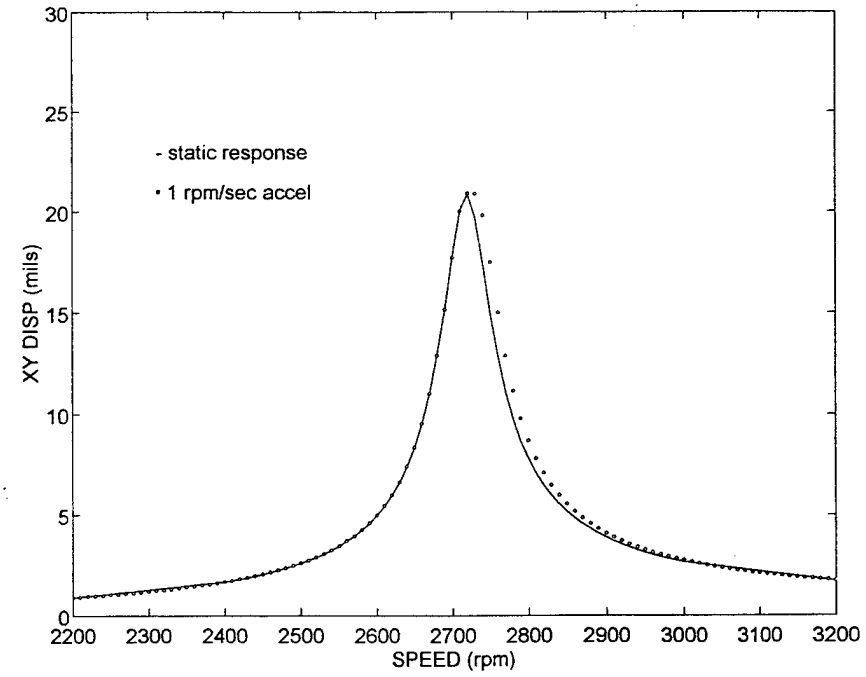

Figure 3. Comparison of the Analytical Model with an Acceleration Rate of 1 RPM/Sec with the Vejvoda Steady State Model.

D. MODEL RESULTS

1. Introduction

Several configurations were run in the numerical models to determine the effect of each of the various parameters on the maximum amplitude of the response. In all cases presented, an imbalance of 1 gram at a distance of 30.5 mm from shaft centerline was used. The system mass used was 0.0061 lbf-sec^2/in, which is the modal mass determined for the experimental facility. When stiffness coefficients were kept constant they were in the region of 495 to 515 lbf/in which is the approximate modal stiffness values determined for the experimental facility. Likewise, when damping was kept constant it was held at a value around 0.04 lbf-sec/in which gives a realistic value of the damping ratio ζ which matches experimental data. Each of the parameters was varied individually to determine its effect on the response. The goal was to determine what factors reduced the maximum response amplitude and/or the duration or number of cycles experiencing high amplitudes.

The displacement curves shown in the plots are the maximum radial displacement, XY given by the formula:

$$XY = \sqrt{\left(x^2 + y^2\right)} \qquad (11)$$

The term XY is used in lieu of the more common terms for radial displacement, r or R to avoid confusion with the Lewis non-dimensional terms (see Figure 4).

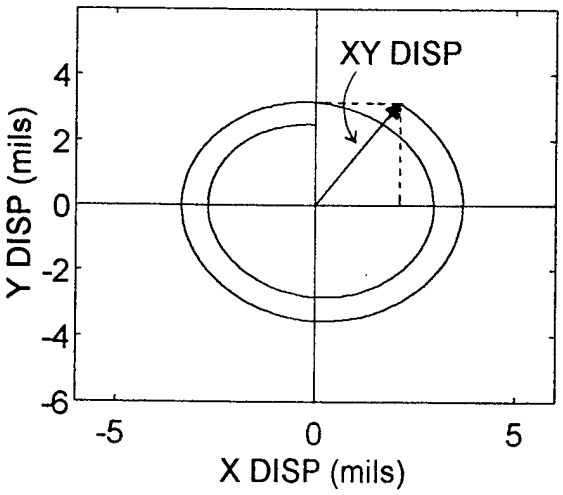

Figure 4. Diagram Showing the Relationship between the Radial Displacement XY and the X and Y Displacement.

2. Determination of number of cycles experienced between $0.9\omega/\omega_n$ and $1.1\omega/\omega_n$.

One of the goals was to minimize the number of cycles experienced at the high vibration levels. To determine the number of cycles occurring between plus or minus 10% of $\omega/\omega_n = 1$, the following formula was derived:

Since,
$$\omega_n = \sqrt{\frac{K}{M}} \tag{12}$$

and the range of ω is from 0.9 to 1.1 ω_n ,

Then,
$$\Delta\omega = \frac{0.2\sqrt{\frac{K}{M}}}{2\pi} \quad \text{(in hertz)} \tag{13}$$

and the time required to traverse this range is given by:

$$t = \frac{\Delta\omega}{h} = \frac{0.2\sqrt{\frac{K}{M}}}{2\pi h} \qquad (14)$$

Where h is the rate of acceleration in cycles per second per second.

The number of cycles experienced while traversing this range can be expressed as:

$$\#\ Cycles = \omega_{\circ} t + \frac{1}{2} h t^2 \qquad (15)$$

Using substitution, the resultant equation is:

$$\#\ Cycles = \frac{0.05K}{\pi^2 Mh} \qquad (16)$$

To put this in terms of q, use the relationships:

$$N = \sqrt{\frac{K}{M}} \Big/ 2\pi \qquad (17)$$

where N is the natural frequency in cycles/sec, and:

$$h = N^2 / q \qquad (18)$$

This gives us a very simple form of the equation:

$$\#Cycles = 0.2q \qquad (19)$$

Equations (13) and (16) give us the number of cycles that occur within plus or minus 10% of $\omega/\omega n = 1$. At high rates of acceleration, the shift in the apparent critical speed can place the region of highest amplitudes out of this range. The number of cycles occurring within the same range around the ω of maximum response will, however, be very close to this same value.

3. Symmetric stiffness and damping at different rates of acceleration.

The maximum displacement-vs-rpm curves for various acceleration rates on a symmetric rotor are shown in Figure 5. K_{XX} and K_{yy} are symmetric at 495 lbf/in and C_{XX} and C_{yy} are equal at 0.04 lbf-sec/in (ζ=.0115). All cross terms are zero. Acceleration rates of 1, 250, 500, 1000, and 2000 rpm/sec were used (these acceleration rates have approximate non-dimensional q values of 123200, 493, 246, 123, and 62 respectively). Just as in the Lewis' curves, these curves show the maximum amplitude decreasing with increasing acceleration rates. The apparent shift of the critical speed is also easily seen in this figure. As the acceleration is doubled from 250 rpm/sec to 500 rpm/sec there is a 12.9% decrease in the maximum amplitude and a 40 rpm increase in the speed of maximum response. As acceleration is again doubled to 1000 rpm/sec, there is an accompanying 15.5% decrease in the maximum amplitude and a increase of 60 rpm. When the acceleration rate is again doubled to 1000 rpm/sec, the maximum amplitude decreases by 19.5% and the increase in the speed of maximum response is 80 rpm.

4. Symmetric stiffness and damping at different rates of deceleration.

The same values for all parameters used in the accelerating case were again used for decelerating at the same rates. Figure 6 shows the corresponding curves for the same rates of deceleration. This shows slightly lower maximums than for the accelerating case. The maximum amplitude is 0.03% lower for the 1 rpm/sec curve and increases to 6.4% lower for the 1000 rpm/sec curve. The trend then reverses and the curve for 2000 rpm/sec deceleration is only 2.9% less then its corresponding acceleration curve. The shift in the apparent critical speed is now to the left and by an amount similar to that seen in the case of acceleration.

5. Effects of stiffness asymmetry

To determine if stiffness asymmetry could be used advantageously to reduce the maximum amplitude, model runs with varying degrees of stiffness asymmetry were made. The effect of varying the stiffness asymmetry on a rotor experiencing acceleration is shown in Figure 7. The acceleration for all curves was held constant at 360 rpm/sec ($q \cong 356$), C_{xx} and C_{yy} were held at 0.04 lbf-sec/in ($\zeta = .0113$), and the stiffness asymmetry was varied from a delta of zero to 70 lbf/in in steps of 10 lbf/in around a mean of 515 lbf/in. All cross terms were zero. With the stiffness symmetric at 515 lbf/in, the maximum amplitude is around 16 mils. As a slight asymmetry of 10 lbf/in is introduced, the maximum jumps to around 19 mils, an increase of almost 19%. As the asymmetry is increased to 20 lbf/in, the maximum increases to almost 21 mils or by 31%. As the asymmetry is further increased, the maximum now starts to decrease due to separation of the split resonance peaks. This split resonance was determined by Vejvoda [Ref. 2] to be one cause of backwhirl. At an asymmetry of 70 lbf/in the maximum amplitude has returned very nearly to the value at zero

asymmetry, however, there are now two distinct critical speeds and a wider range of rpms in which the amplitude of the response is significant.

To determine if the trend is the same in the steady state case of zero acceleration, the same values were run in the Vejvoda model and the results are shown in Figure 8. The trend appears to be the same regardless of whether the rotor is accelerating or not.

6. **Effects of a cross stiffness term.**

In order to determine the effects of a cross stiffness term, acceleration was held constant at 360 rpm/sec ($q \cong 356$), C_{XX} and C_{yy} at 0.04 lbf-sec/in ($\zeta = .0113$), K_{XX} and K_{yy} were held constant at 515 lbf/in, and K_{yX} was varied from zero to 30 lbf/in. K_{Xy} and the damping cross terms were held at zero. The results are shown in Figure 9. The cross stiffness term appears to have no significant effect on the maximum amplitude of the accelerating rotor until it reaches a value of 30 lbf/in. It then has a very significant effect, increasing the maximum by nearly 40% as well as shifting the apparent critical speed to the right. In addition, starting at a value of K_{yX} = 10 lbf/in, this cross term induced backwhirl in the accelerating rotor model. The rotor orbit from 2860 to 2875 rpm showing the onset of backwhirl is shown in Figure 10.

Again, to determine if the trend is the same in the psuedo-static case of zero acceleration, the same values were ran in the Vejvoda model and the results are shown in Figure 11. In the case of zero acceleration, the results were very different. Unlike in the accelerating case, the cross term introduced in the pseudo-static case had a significant effect on the maximum amplitude for each value of K_{yX}. As the value of the cross term increased, so did the amplitude of the response. However, this did not induce backwhirl in the static model and produced no significant shift in the apparent critical speed.

An additional run was made was made with an acceleration rate of 16.67 rpm/sec (q≅7689) and as can be seen in Figure 12, these curves begin to show the same trend as in the case of zero acceleration.

7. Effects of symmetric damping.

Although its effects are well documented, symmetric damping was evaluated for an accelerating rotor in the numeric model and the results are shown in Figure 13. The acceleration rate was held constant at 360 rpm/sec (q≅342), K_{XX} and K_{yy} were held at 495 lbf/in and symmetric damping was evaluated at zero, 0.02, 0.04, and 0.08 (ζ=0, 0.0058, 0.0115 and 0.0230). All cross terms were zero. As expected from the Lewis analysis, the amplitude of the maximum response decreases significantly with an increase in damping.

8. Effects of damping asymmetry.

The effect of varying the degree of damping asymmetry on a rotor experiencing acceleration is shown if Figure 14. The acceleration for all curves was held constant at 360 rpm/sec (q≅356), K_{XX} and K_{yy} were held at 515 lbf/in, and the damping asymmetry was varied from a delta of zero to 0.05 lbf-sec/in in steps of 0.01 lbf-sec/in around a mean of 0.04 lbf-sec/in (ζ=0.0113). All cross terms were zero. With each increase in the amount of damping asymmetry, there was an accompanying increase in the amplitude of the maximum response of 6 to 10%. This maximum value was the same as what would be obtained by having symmetric damping at the lower value. That is, if C_{XX} = 0.065 and C_{yy} = 0.015, the resulting maximum amplitude is the same as would be observed with C_{XX} = C_{yy} = 0.015. This trend did not reverse as it did in the asymmetric stiffness case. This asymmetric damping also induced backwhirl. The rotor orbit from 2885 to 2900 rpm displaying the onset of the backwhirl is shown in Figure 15.

When compared with the zero acceleration runs made in the Vejvoda model (see Figure 16), the trend appears to be the same. However, there is no induced backwhirl in

the zero acceleration model. It therefore appears that damping asymmetry can induce backwhirl in an accelerating rotor but not in a steady state rotor.

9. **Effects of acceleration changes.**

While studying the responses from the numerical model at different rates of acceleration, the question arose as to whether acceleration scheduling could be used to minimize the response of the rotor. The possibility of taking advantage of the apparent shift in the critical speed at high rates of acceleration was explored. The idea was to start at a high rate of acceleration which would cause a shift in the critical speed to the right. After the rotor is past what would be the critical speed at a lower rate of acceleration, but before the rotor reaches the critical speed at its present higher acceleration, the acceleration would be immediately slowed to the lower rate. The question was, would this "fool" the rotor into thinking that it was already past its critical speed and therefore would the amplitude start decreasing to give a maximum less than what it would have been if the acceleration were left at the higher rate. Figure 17 shows this more clearly.

A numerical model was modified to allow for one instantaneous change in acceleration with the rpm at which the change was to occur entered as a variable. This model was limited in that it gave an unrealistic instantaneous change in acceleration, that is:

$$\ddot{\theta} = \ddot{\theta}_1 (t < t_o) \tag{20}$$

$$\ddot{\theta} = \ddot{\theta}_2 (t > t_o) \tag{21}$$

and that it did not allow for any complex scheduling of acceleration in that $\theta(t)$ was not specified.

Figure 18 shows the results of one of these change acceleration runs. The stiffness values were K_{xx} and K_{yy} = 495 and the damping values were C_{xx} and C_{yy} = 0.04

(ζ=0.0115). The initial acceleration was 2000 rpm/sec (q≅62) which was switched to 250 rpm/sec (q≅493) at an rpm of 2870. The figure shows the results of the run along with plots of the 250 and 2000 rpm/sec acceleration response curves. As can be seen, the amplitude of the response is only slightly less than that of the continuous 2000 rpm/sec acceleration response. However, the response does "ring down" much more rapidly yielding fewer cycles at the higher vibration levels.

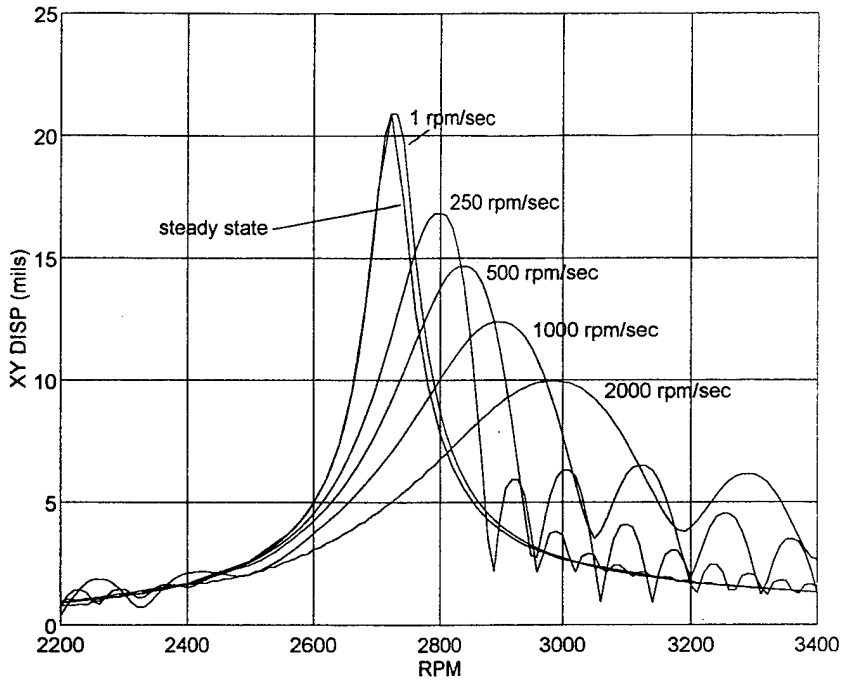

Figure 5. Symmetric Stiffness and Damping at Various Acceleration Rates (Kxx=Kyy=495 lbf/in, Cxx=Cyy=0.04 lbf-sec/in, All Cross Terms are Zero).

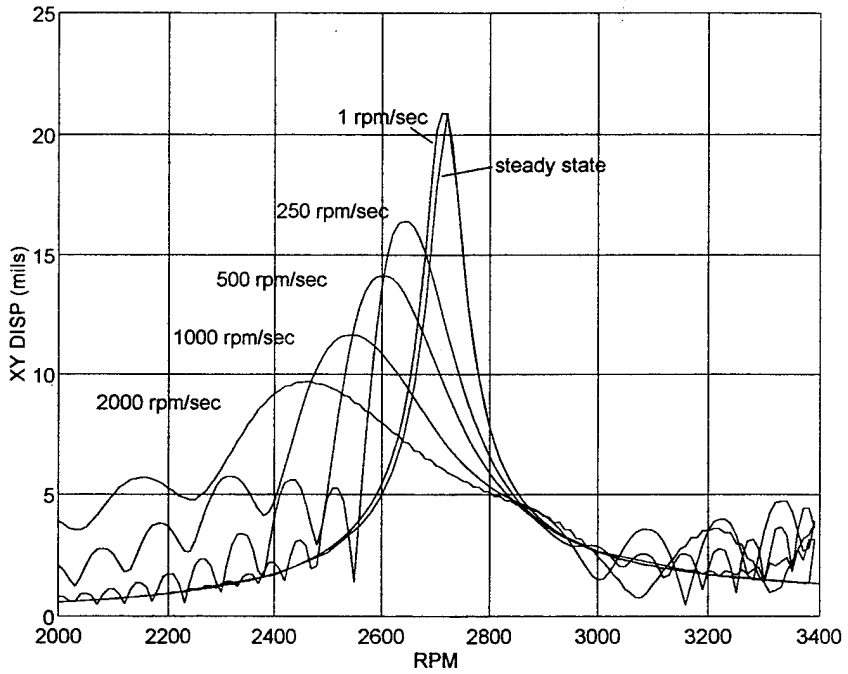

Figure 6. Symmetric Stiffness and Damping at Various Deceleration Rates (Kxx=Kyy=495 lbf/in, Cxx=Cyy=0.04 lbf-sec/in, All Cross Terms are Zero).

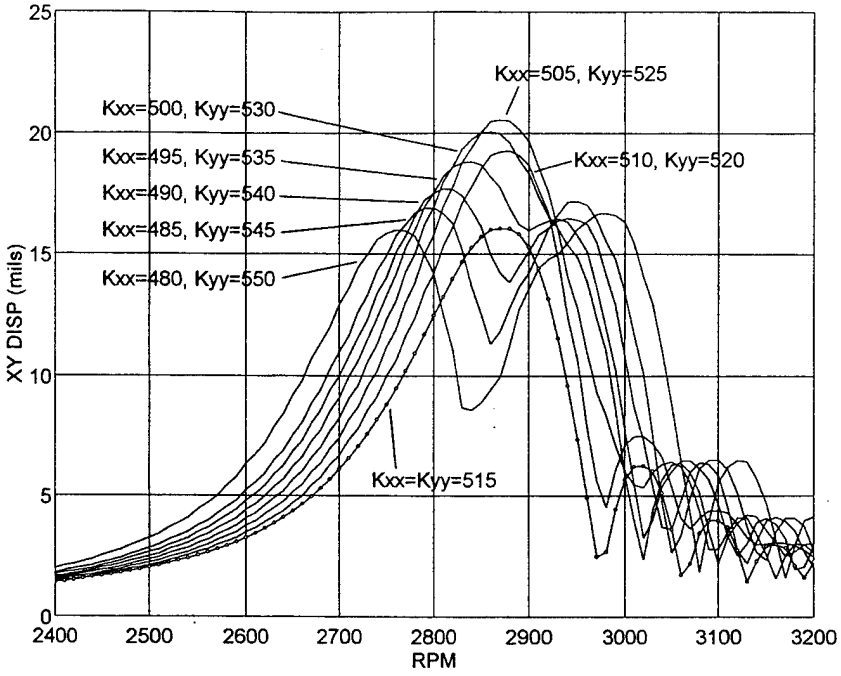

Figure 7. Effects of Stiffness Asymmetry around a Mean of 515 lbf/in (Cxx=Cyy=0.04 lbf-sec/in, All Cross Terms are Zero, Acceleration Rate is 360 RPM/Sec).

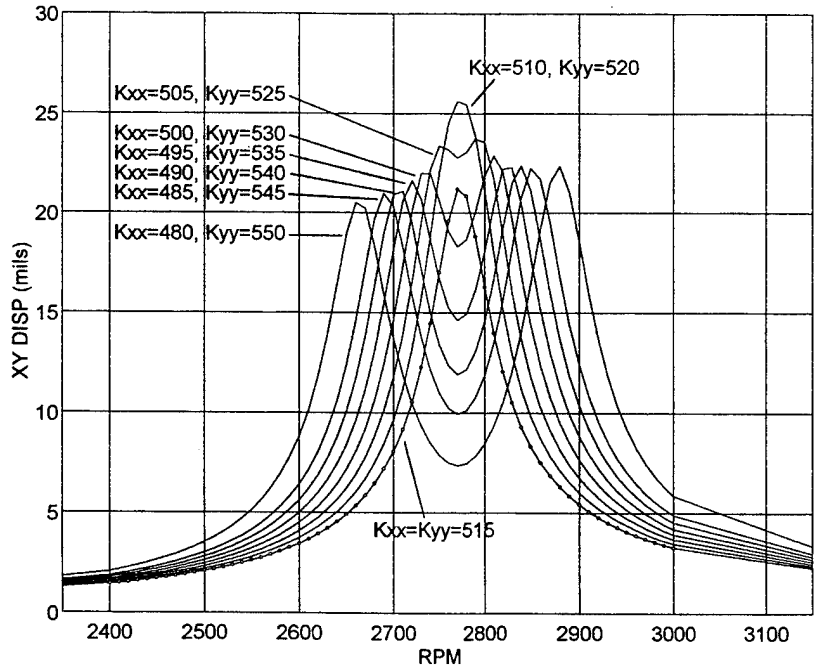

Figure 8. Effects of Stiffness Asymmetry around a Mean of 515 lbf/in in the Steady State Model (Cxx=Cyy=0.04 lbf-sec/in, All Cross Terms are Zero).

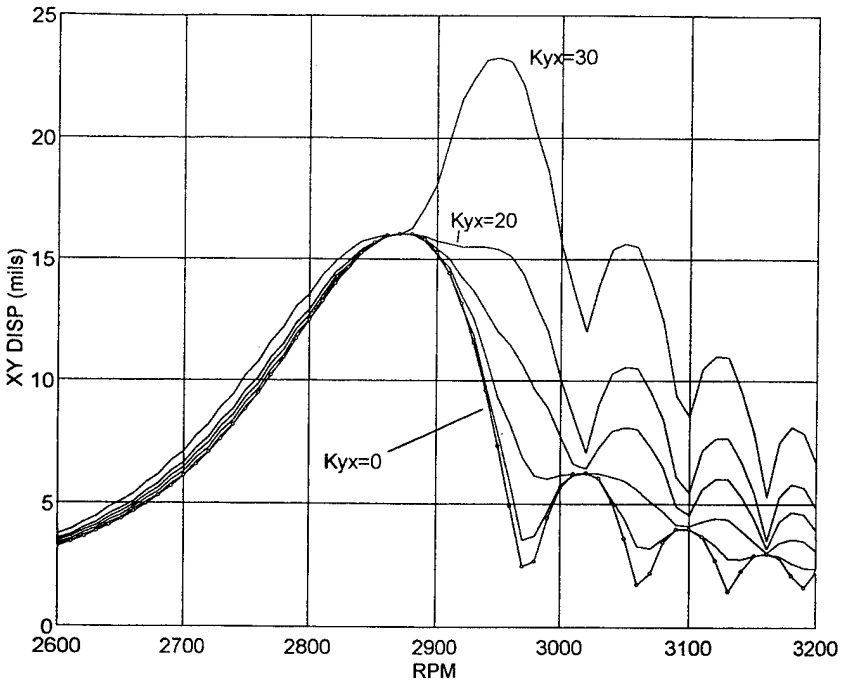

Figure 9. Effects of a Stiffness Cross Term (Cxx=Cyy=0.04 lbf-sec/in, Kxy and Damping Cross Terms are Zero, Acceleration Rate is 360 RPM/Sec).

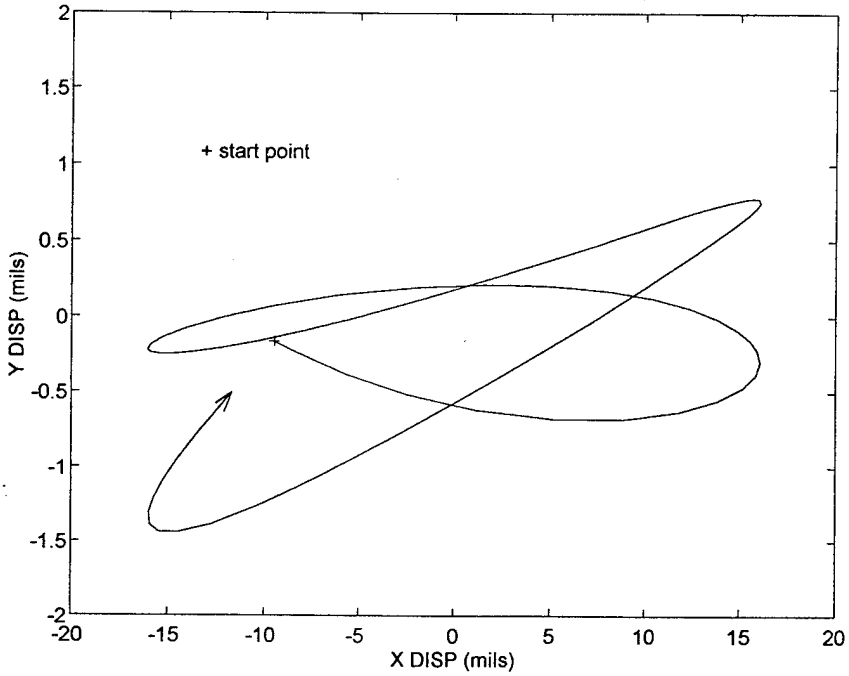

Figure 10. Rotor Orbit Showing the Onset of Backwhirl between 2860 and 2875 RPM due to a Stiffness Cross Term (Cxx=Cyy=0.04 lbf-sec/in, Kxy and Damping Cross Terms are Zero, Acceleration Rate is 360 RPM/Sec).

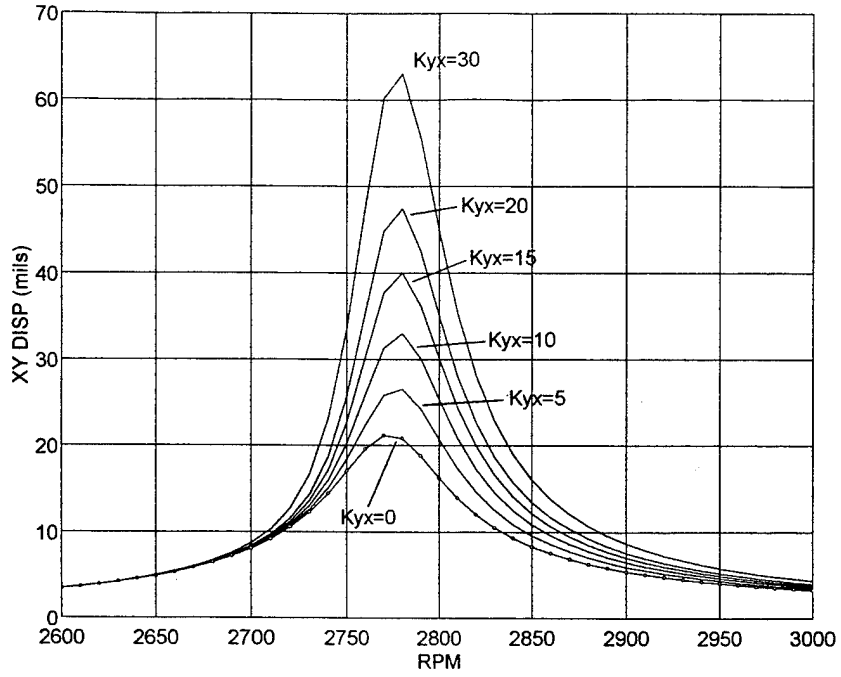

Figure 11. Effects of a Stiffness Cross Term in the Steady State Model (Cxx=Cyy=0.04 lbf-sec/in, Kxy and Damping Cross Terms are Zero).

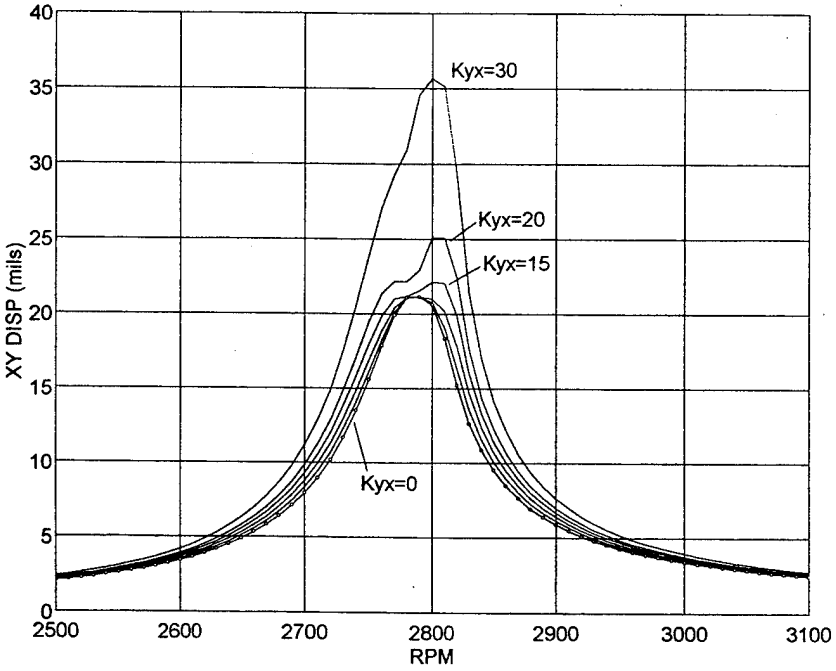

Figure 12. Effects of a Stiffness Cross Term (Cxx=Cyy=0.04 lbf-sec/in, Kxy and Damping Cross Terms are Zero, Acceleration Rate is 16.67 RPM/Sec).

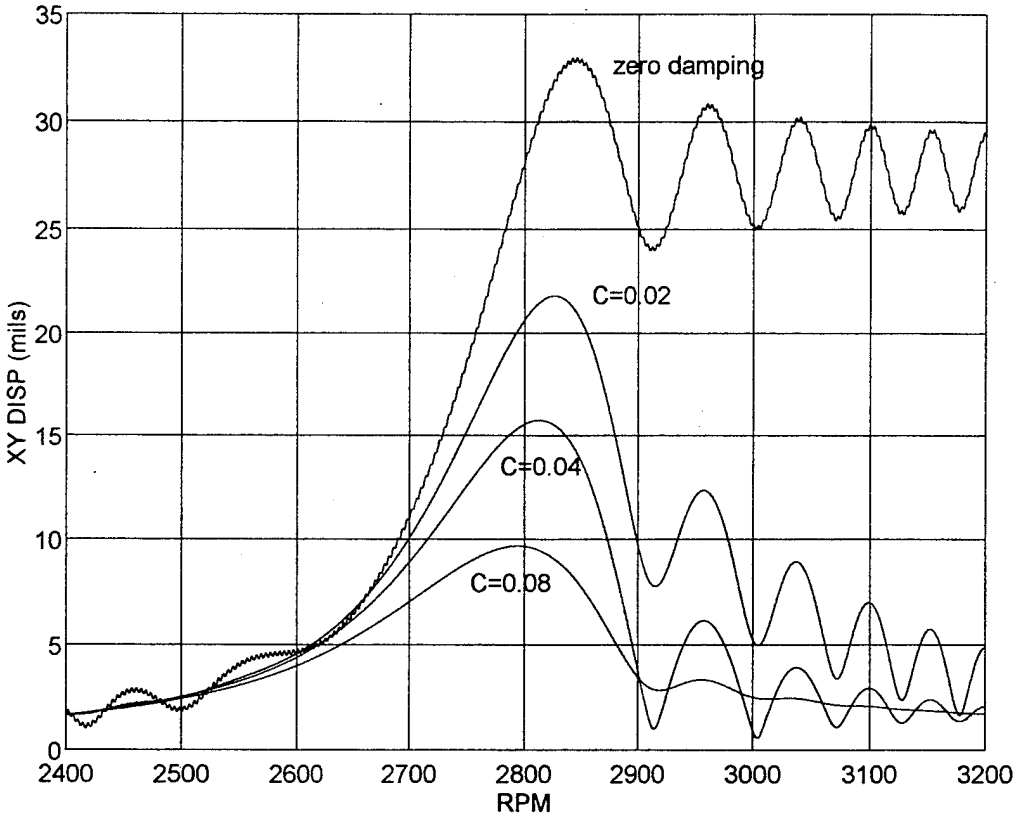

Figure 13. Effects of Symmetric Damping (Kxx=Kyy=495 lbf/in, all Cross Terms are Zero, Acceleration Rate is 360 RPM/Sec).

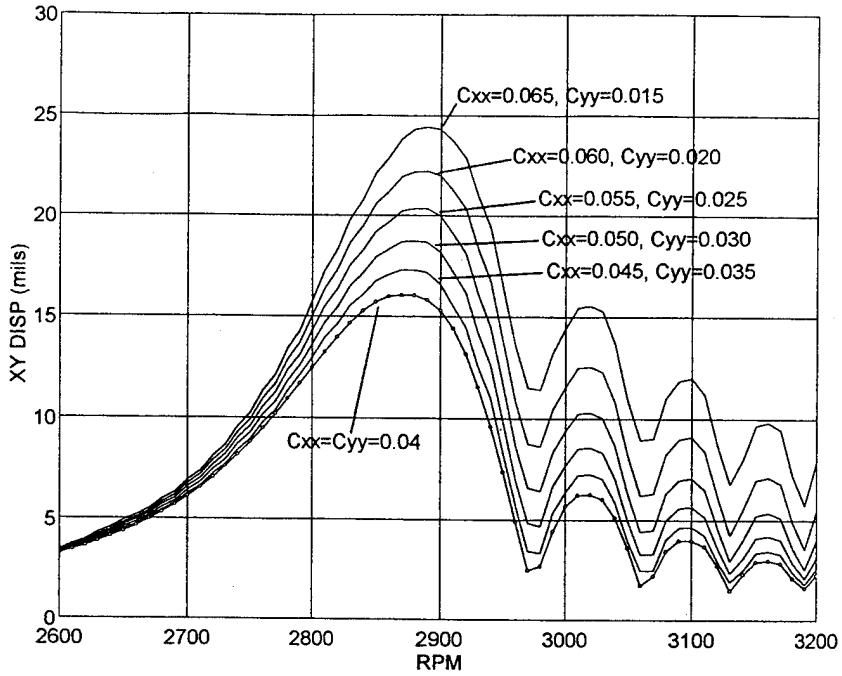

Figure 14. Effects of Damping Asymmetry around a Mean of 0.04 lbf-sec/in (Kxx=Kyy=515 lbf/in, All Cross Terms are Zero, Acceleration Rate is 360 RPM/Sec).

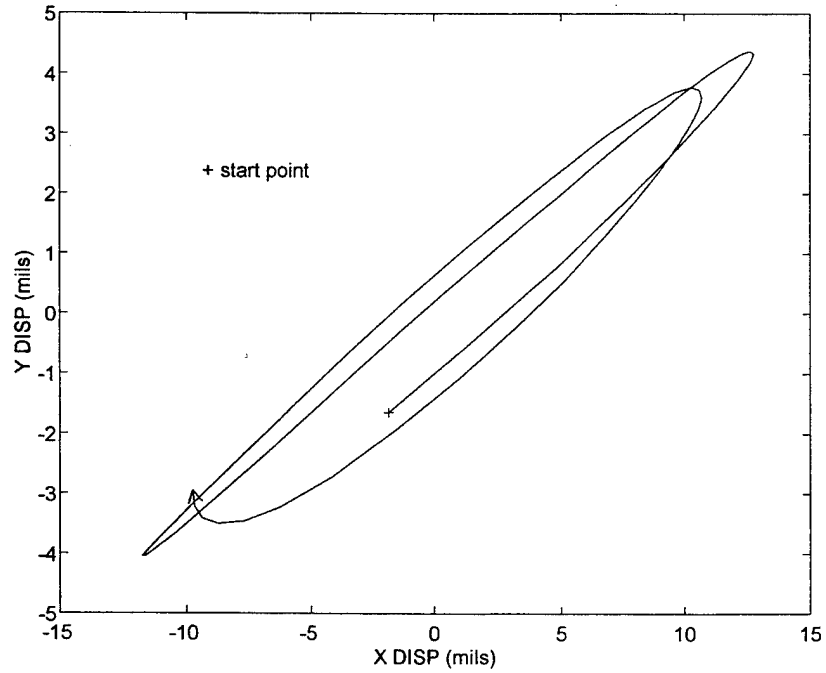

Figure 15. Rotor Orbit Showing the Onset of Backwhirl between 2885 and 2900 RPM due to Damping Asymmetry (Kxx=Kyy=515 lbf/in, All Cross Terms are Zero, Acceleration Rate is 360 RPM/Sec).

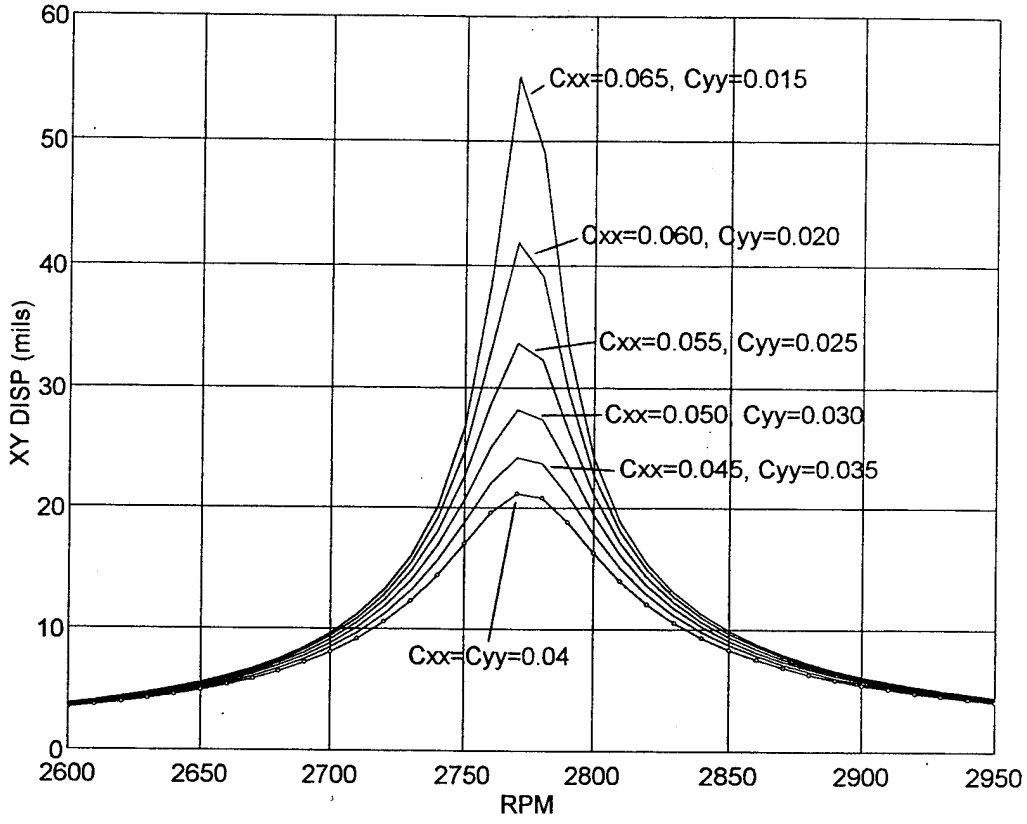

Figure 16. Effects of Damping Asymmetry around a Mean of 0.04 lbf-sec/in in the Steady State Model (Kxx=Kyy=515 lbf/in, All Cross Terms are Zero, Acceleration Rate is 360 RPM/Sec).

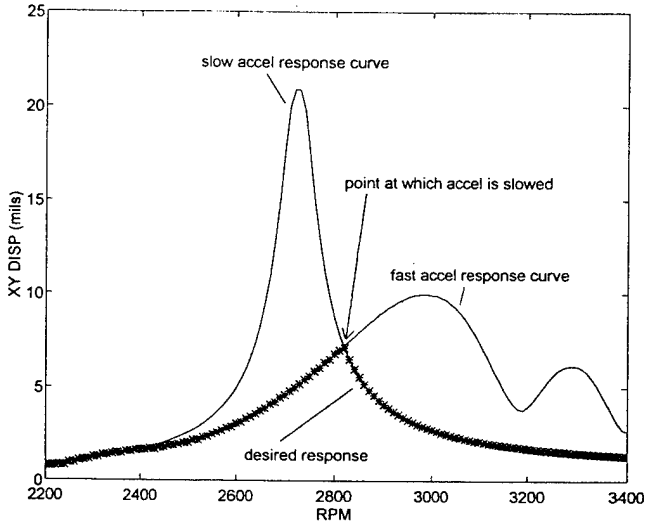

Figure 17. Representation of how the Shift in the Apparent Critical Speed may be used to reduce Maximum Rotor Response.

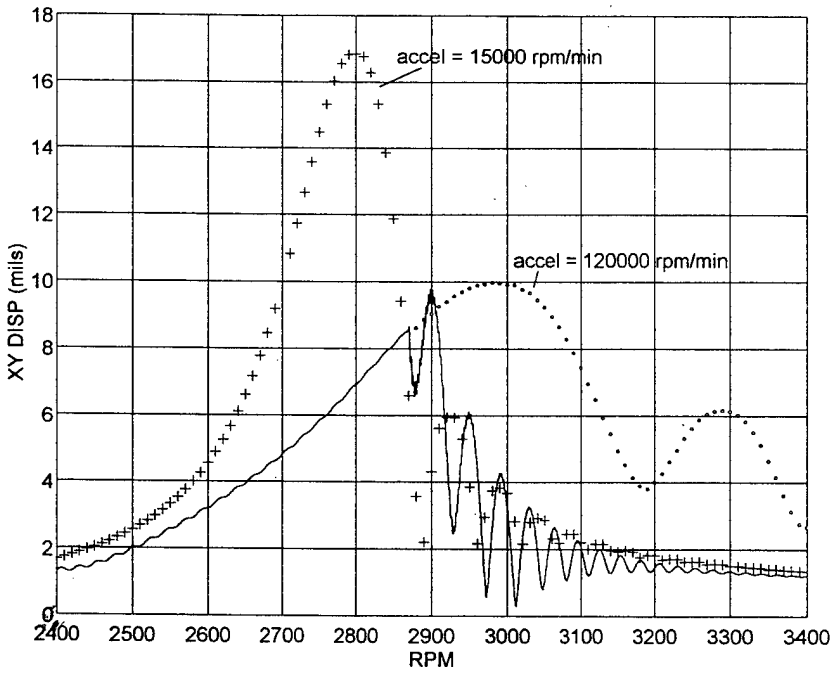

Figure 18. Results of Instantaneously Changing the Acceleration Rate (Kxx=Kyy=495 lbf/in, Cxx=Cyy=0.04 lbf-sec/in, All Cross Terms are Zero).

IV. EXPERIMENTAL INVESTIGATION

A. EXPERIMENTAL FACILITY

1. Introduction

The experimental facility used consisted of the Bentley Nevada rotor kit and Labview software used by both Simei [Ref. 12] and Vejvoda (Ref. 2]. However, several updates and or changes were made to the facility. Figures 19 through 21 show photographs of the facility.

2. Upgrade to Pentium

The DataStor IBM personal computer used for data acquisition was replaced with a Unitek personal computer with a Pentium chip and a CPU speed of 66MHz. The National Instruments Data Acquisition Interface Board (AT-MIO-16F-5) is the same.

3. Table Mounting

In both Simei's and Vejvoda's experiments, the rotor kit was placed on a foam pad sitting on an ordinary table. In Vejvoda's experiments with the kit mounted in the vertical and wall mounted horizontal planes, the rotor kit was mounted to a non-structural wall of the laboratory. The vibrational characteristics of these mountings and therefore the effects they had on the rotor response were unknown. It is desirable to have the capability to firmly mount the rotor kit in any one of the three orientations with respect to gravity on a table with a natural frequency which is much lower than the frequency of the forcing function which might be experienced by the imbalanced rotor. In this way, the mounting table will not be excited by the imbalanced rotor and therefore, will not effect the response of the rotor.

A heavy steel table was designed for the rotor lab and is shown in Figures 19, 20, and 21 with the rotor kit placed in the flat horizontal, wall mounted horizontal, and vertical mounting positions respectively. The weight of the table is 266 lbs without the rotor kit and it is supported by four Barry 6E100 machinery mounts which have a very low stiffness (each rated at 5.4 to 8.1 Hz for loads of 50 to 100 lbf). This provides for a natural frequency of less than 8 Hz in both the axial and radial directions.

4. Optical Encoder and Frequency Divider

The Labview program ROTOR.VI used by Simei and Vejvoda used a data acquisition scan rate of 4096 scans/sec. This scan rate was constant regardless of rotor speed, therefore the exact position of the shaft when each acquisition was made was not controlled. It is preferable to know the position of the shaft at each acquisition for the purpose of phase locking and ensemble averaging. To accomplish this, a Hewlett Packard HEDS5540 optical encoder was attached to the end of the drive motor shaft. This encoder outputs 256 pulses per shaft revolution. This output is sent to a frequency divider which was installed on the National Instrument general-purpose termination breadboard (SC-2070). This frequency divider takes the 256 pulse/rev signal and converts it to either a 128, 64, 32, or 16 pulse/rev signal. This output is then connected to the breadboard's OUT2 terminal to be used as an external clocking signal. The ROTOR.VI program has been modified to use this external clocking signal for data acquisition vice the internal scan rate. A complete wiring diagram of the experimental facility which includes the frequency divider connections for the desired scans per revolution is shown in Figure 22.

5. Additional Labview Programs

Some additions and modifications were made to the Labview data acquisition programs to enhance the usability of the lab.

ROTOR2.VI is a program identical to the ROTOR.VI described in [Ref. 12] with the exception of writing the data to a file. Placing this program into continuous run allows the user to observe real time data on the running rotor kit without filling up a data file. This can be used much like an oscilloscope to observe the current rotor orbit and y displacement versus time plots.

ACC ROTOR.VI is a Labview program which allows data acquisition on an accelerating rotor. This program basically places the ROTOR.VI program into a while loop but has also added a stop button and a filename input to the control panel. This program will continue to write data to a file during acceleration until the stop control is activated. This is the program that was used to take the experimental data discussed later in this chapter.

RPM.VI is a Labview program which utilizes the AM9513 clock circuits in the data acquisition board to determine the frequency of the external clocking signal. Since the optical encoder provides a set number of clocking signals per revolution, the program can determine the shaft rpm and thereby eliminate the need for the stroboscope. This is very useful in instantaneously knowing the approximate shaft speed and acceleration but it was found that the last digit of the readout changes at such a rapid rate that it is difficult to read the exact rpm.

COUNTER SUB.VI is a Labview program which similarly uses the AM9513 clock circuits to determine the time interval between the external clocking signals and write the interval to a file. This program was written to be used in conjunction with the ACC ROTOR.VI. It was desired to be able to obtain x, y, and time interval data during an accelerating run. In this way, the actual acceleration rate could be determined and the exact rpm at each acquisition could be determined. Attempts to merge these programs or to run them simultaneously were unsuccessful using Labview version 3.1, probably due to both programs trying to access the same registers simultaneously.

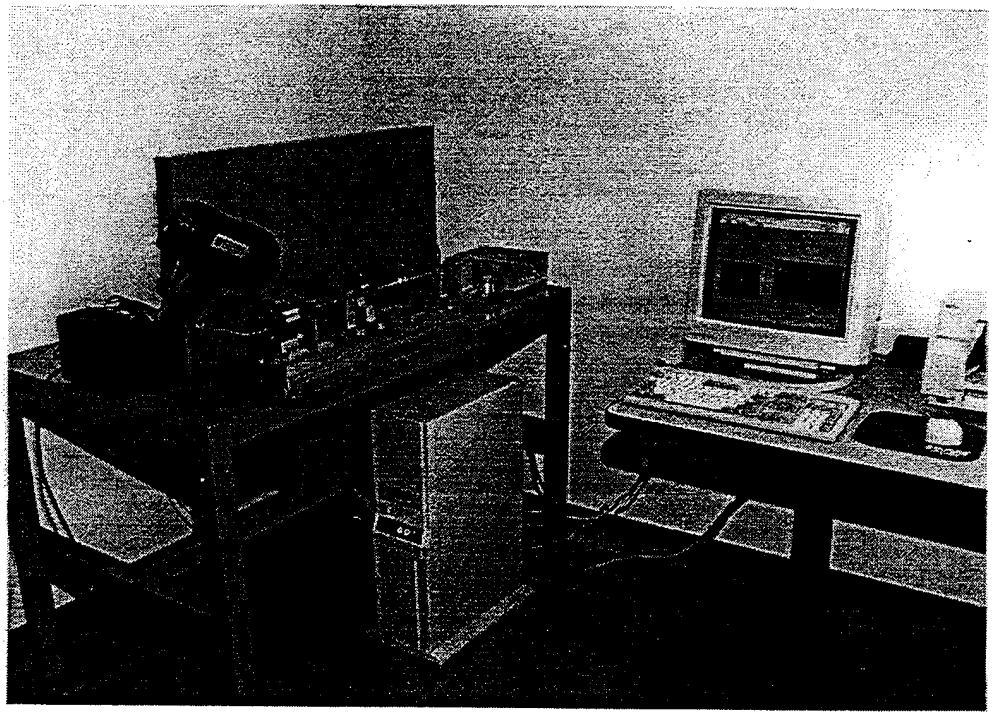

Figure 19. Photograph of Lab Facility with the Rotor Mounted in the Flat Horizontal Position.

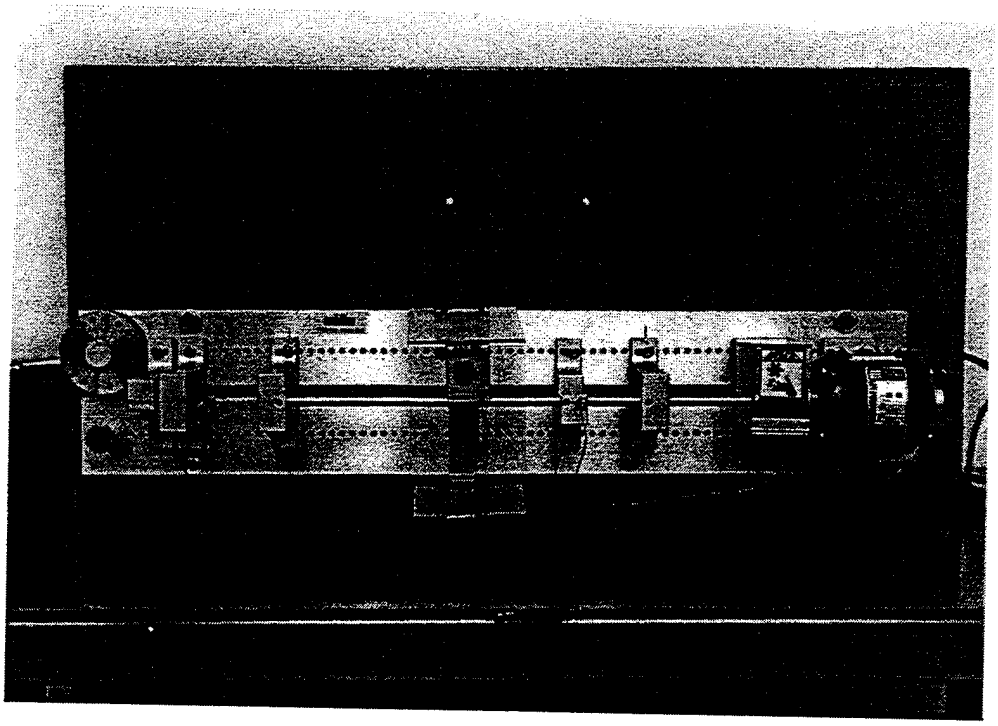

Figure 20. Photograph Showing the Rotor Kit in the Wall Mounted Horizontal Position.

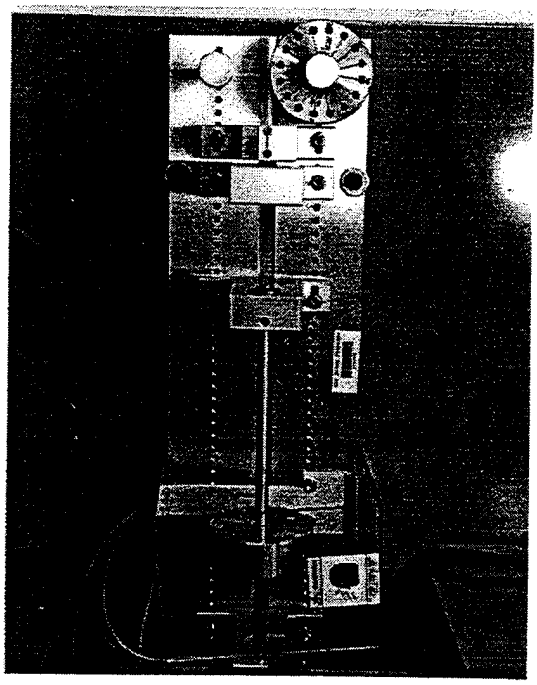

Figure 21. Photograph Showing the Rotor Kit Mounted in the Vertical Position.

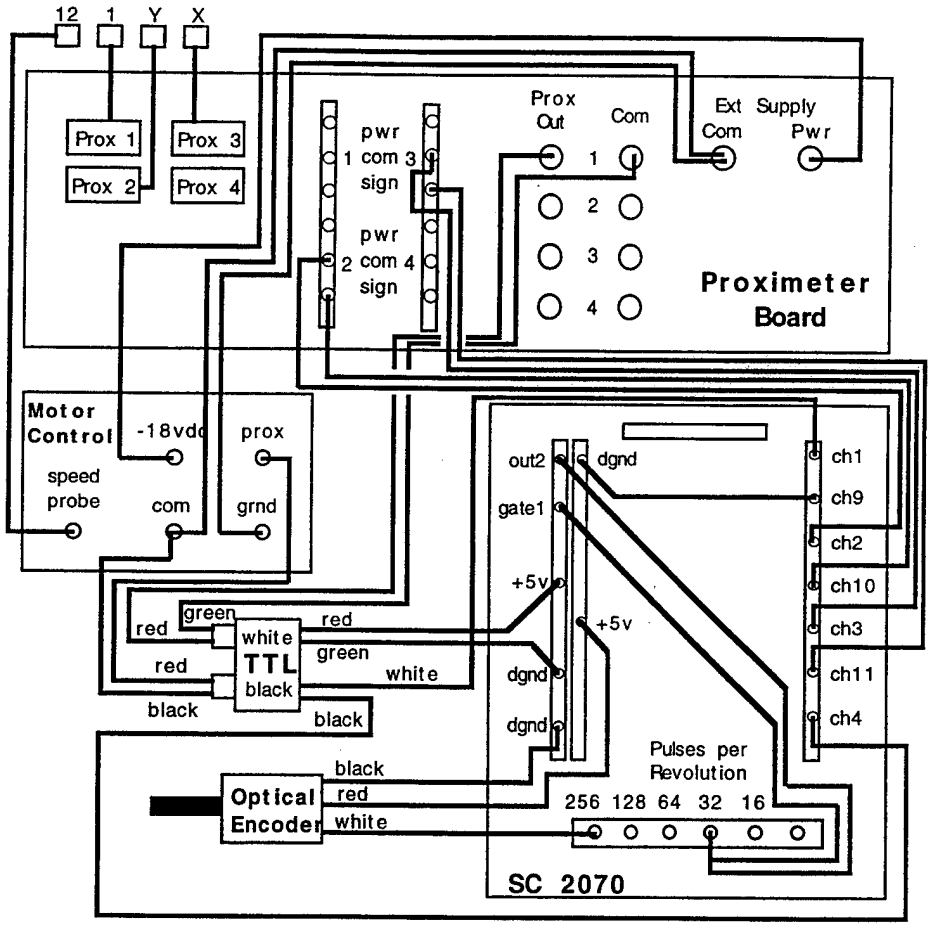

Figure 22. Experimental Facility Wiring Diagram and Frequency Divider Connections.

B. EXPERIMENTAL RESULTS

1. Analysis of the table mounting

The first experiments conducted with the rotor kit mounted on the new table consisted of rerunning some of those made in [Ref. 2]. Vejvoda had determined approximate stiffness and damping coefficients for all three planes of reference experimentally. To determine if his mounting had affected those values, or if the present table mounting changed the values, the zero acceleration runs in all three planes were repeated. The experimental configuration was the same as shown in Figure 5 of [Ref. 2]. Figure 23 shows the results of the flat horizontal run using 1 gram imbalance and a plot of the Vejvoda analytical model results for the K and C values given. Figures 24 and 25 show the same for the wall mounted and vertical runs respectively. The stiffness and damping coefficients have changed considerably with the rotor kit mounted on the heavy, resiliently mounted table. In addition, there was no backwhirl observed in the flat horizontal position as was observed in Vejvoda's experiments.

2. Constant Acceleration runs

The experimental set-up was not as flexible as the numerical model in that the stiffness and damping values could not be readily controlled. However, the motor controller for the rotor kit did allow for control of constant acceleration rates up to 15000 rpm/min within an advertised accuracy of 10 percent. Several runs were made in the flat horizontal mounting position using 1 gram imbalance and acceleration rates of 3000, 6000, 9000, 12000, and 15000 rpm/min. Figures 26 through 30 show experimental results against the numerical predictions using the K and C values determined in the previous paragraph. Since the rpm at which the response occurred in the experimental data could not

be determined using our present data acquisition system, the maximum amplitudes are what is of interest. Some results are tabulated in Table 1.

Table 1. Sample of Experimental Results

Acceleration Rate (rpm/min)	**Max Amplitude of Model** (mils)	**Max Experimental Amplitude** (mils)	**% Error**
3000	13.29	13.41	< 1%
6000	13.21	13.3	< 1%
9000	13.05	13.09	< 1%
12000	12.87	13.09	1.7%
15000	12.67	12.77	< 1%

The experimental values of the maximum amplitude obtained were slightly higher than in the model for all rates of acceleration. The decreasing trend in the amplitude of the maximum response as acceleration is increased matches very closely with the numerical model. The experimental data was within 2% of the analytical in all cases and varied less than 1% for most.

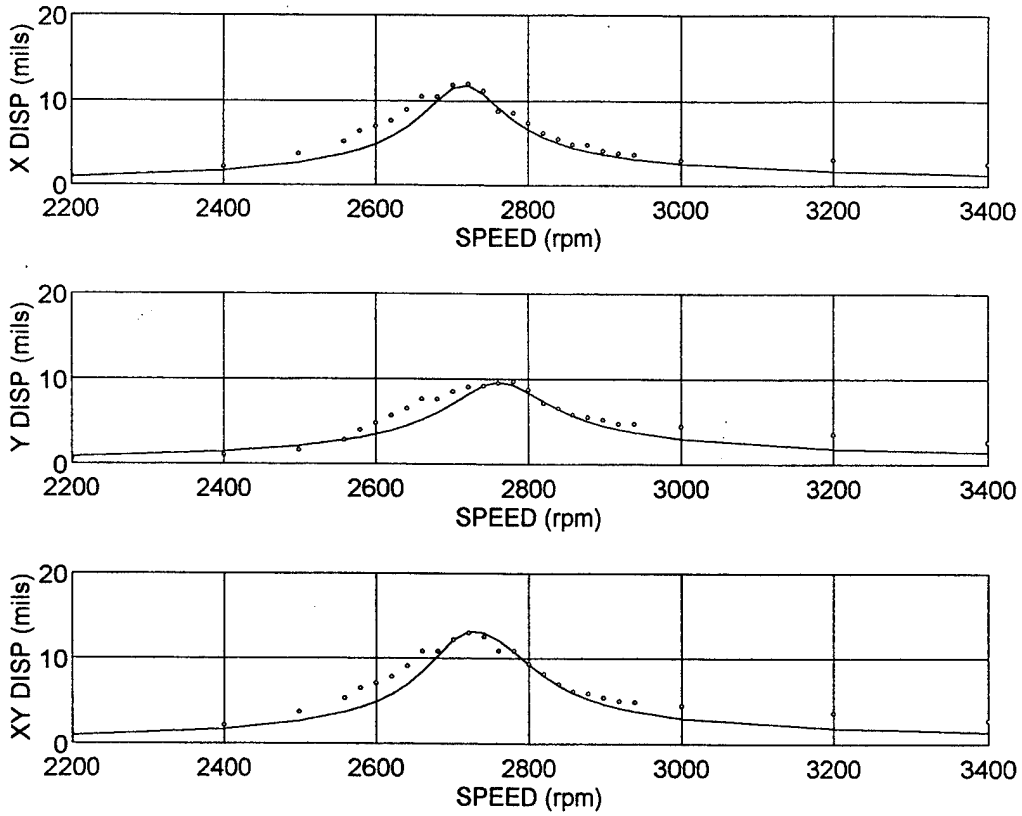

Figure 23. Experimental and Theoretical X Displacement, Y Displacement, and XY Displacement Steady State Data (Kxx=493, Kyy=510, Cxx=0.07, Cyy=0.088, All Cross Terms are Zero (Flat Horizontal Mounting)).

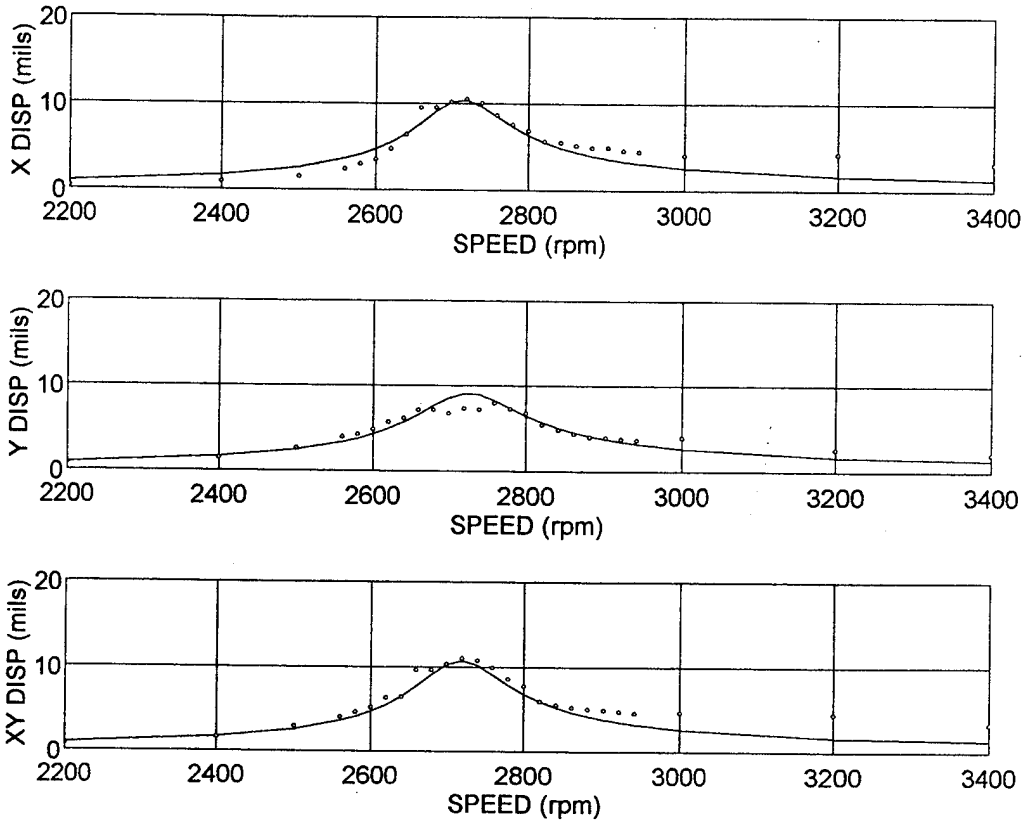

Figure 24. Experimental and Theoretical X Displacement, Y Displacement, and XY Displacement Steady State Data (Kxx=493, Kyy=497, Cxx=0.08, Cyy=0.092, All Cross Terms are Zero (Wall Mounted Horizontal)).

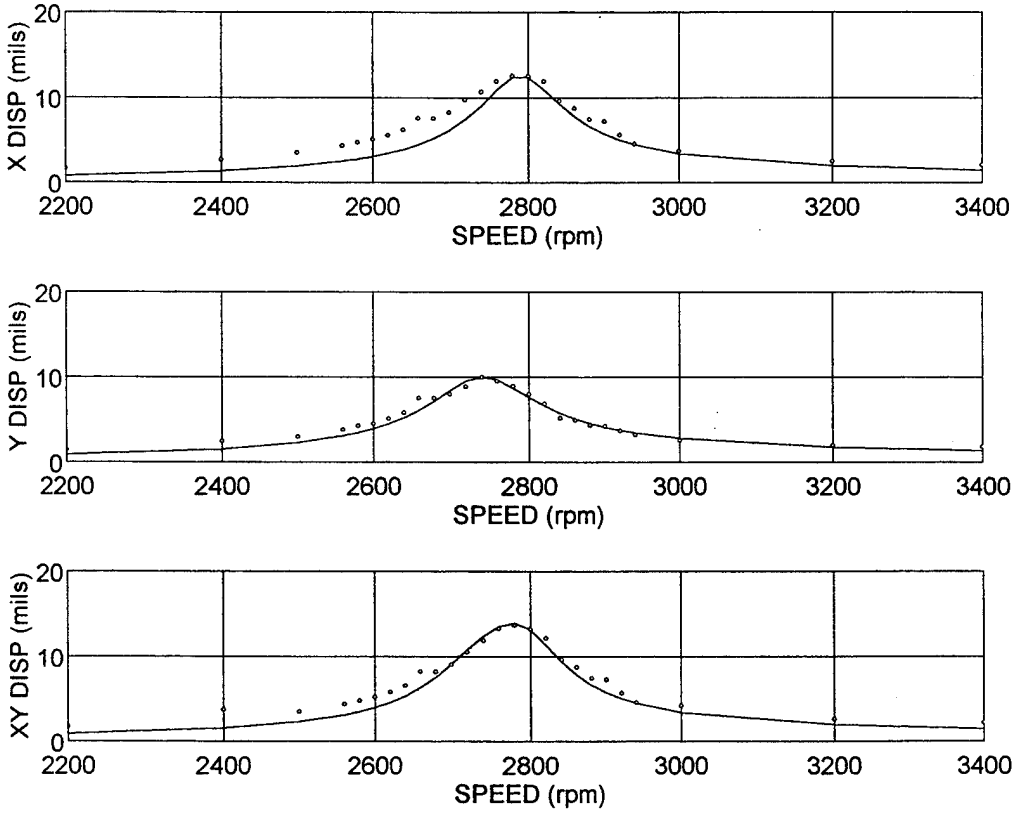

Figure 25. Experimental and Theoretical X Displacement, Y Displacement, and XY Displacement Steady State Data (Kxx=521, Kyy=503, Cxx=0.068, Cyy=0.084, All Cross Terms are Zero (Vertical Mounting)).

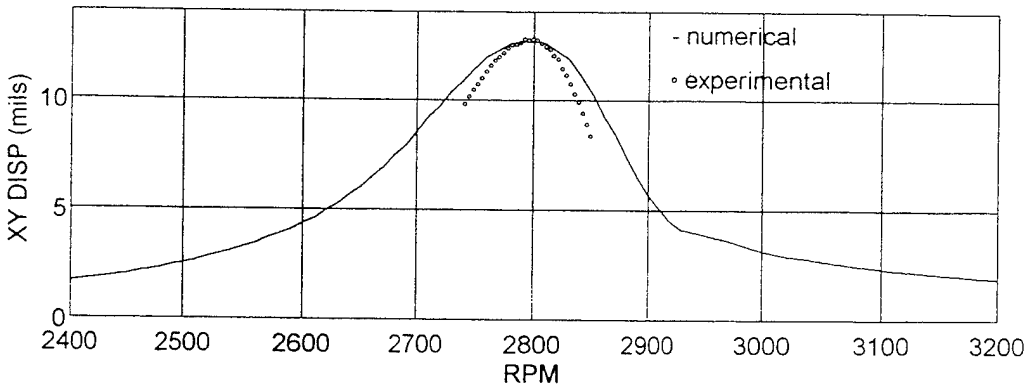

Figure 26. Experimental -vs- Theoretical Maximum XY Displacement Plot (Acceleration rate is 15000 RPM/Min).

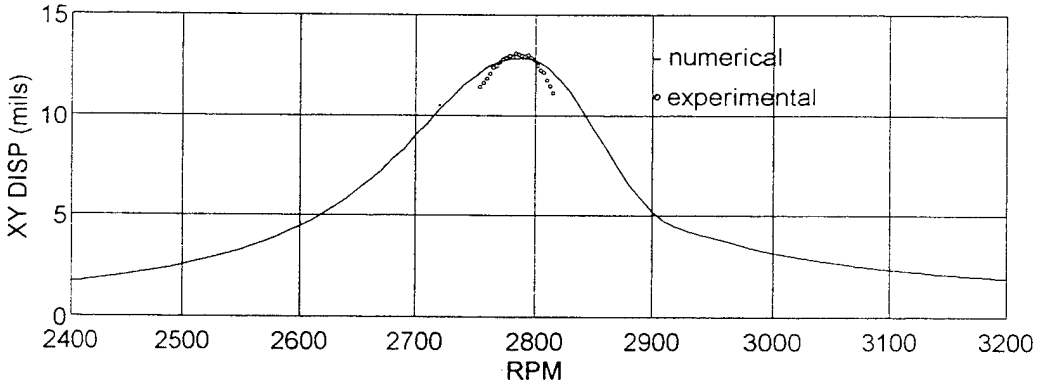

Figure 27. Experimental -vs- Theoretical Maximum XY Displacement Plot (Acceleration rate is 12000 RPM/Min).

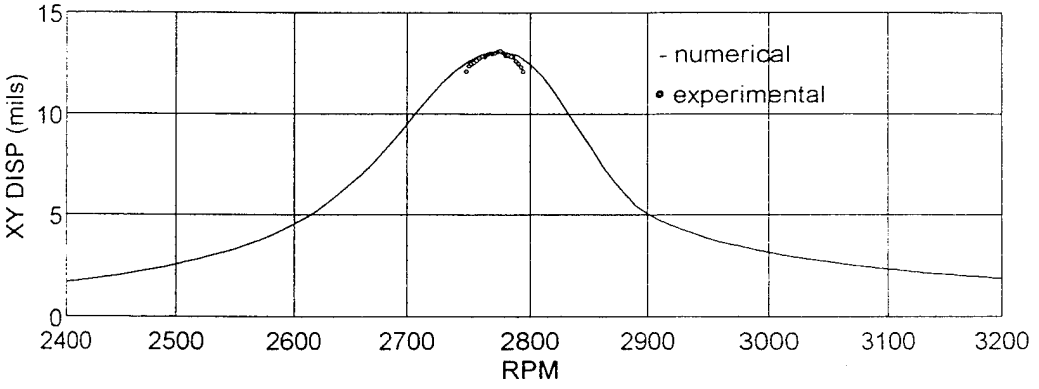

Figure 28. Experimental -vs- Theoretical Maximum XY Displacement Plot (Acceleration rate is 9000 RPM/Min).

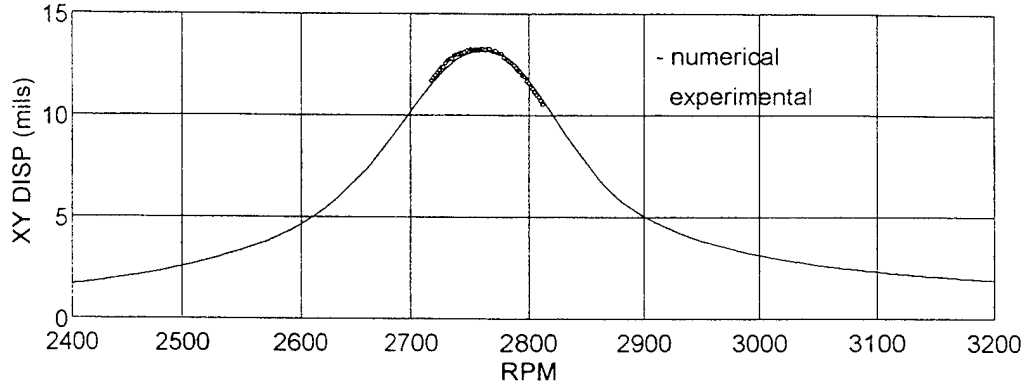

Figure 29. Experimental -vs- Theoretical Maximum XY Displacement Plot (Acceleration rate is 6000 RPM/Min).

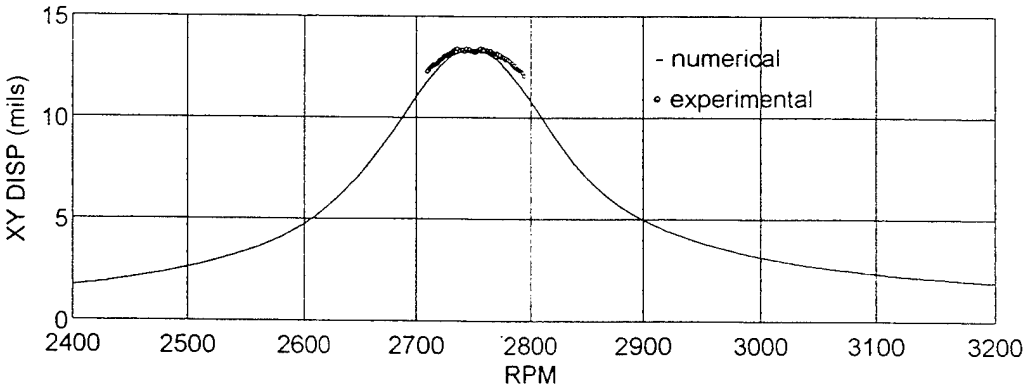

Figure 30. Experimental -vs- Theoretical Maximum XY Displacement Plot (Acceleration rate is 3000 RPM/Min).

V. DISCUSSION OF RESULTS

Both the computer model and the experimental data reveal that increases in the rate of acceleration and the amount of damping have the greatest effect on reducing the amplitude of the response of the rotor passing through it first lateral bending critical speed. The rate of acceleration must be relatively large to have a significant effect on reducing the maximum amplitude of the response. Lewis [Ref. 1] considered a q value of 500 to still be a rather slow rate of acceleration. This analysis showed in Figure 5 that a q value of almost 500 still gave a noticeable reduction of greater than 12 percent in the amplitude of the maximum response. Therefore the acceleration should give a q value of less than 500 to have notable effects. If these large accelerations can be achieved, they are possibly the easiest way to significantly reduce the magnitude of the response.

Acceleration introduces other phenomena as well. In addition to the apparent shift in the critical speed during acceleration, the analysis also uncovered that acceleration can generate backwhirl under conditions in that it would not be generated with little or no acceleration. This was predicted by the model in both the case of a cross-stiffness term and in the case of direct damping asymmetry. Another effect of acceleration is that the whirling is not synchronous and therefore the phase shift of the mass imbalance transitioning from the outside to the inside of the orbit as the rotor passes through critical is no longer evident. This non-synchronous whirling can lead to fatigue in the rotor shaft. The benefit of reducing the maximum response due to a high rate of acceleration, however, outweighs the detriments.

Increased damping is another highly effective means to keep the relative maximum amplitudes low, though it is much more difficult to predict and to control. The assessment

of asymmetric damping revealed that for lateral bending, the total damping is only as good as the least amount of damping in the system. Asymmetric damping is not beneficial.

Much like perfect balance, perfect symmetry in a real system is difficult if not impossible to achieve. The analysis shows that small amounts of stiffness asymmetry can substantially increase the maximum amplitude of the rotor response, yet, as the asymmetry increases, the amplitudes reach a point where they start to decrease and can be reduced roughly to the amplitudes found with perfect symmetry. If nearly perfect stiffness symmetry cannot be achieved, it may be a better choice to design further stiffness asymmetry into the system to bring down the amplitude of the maximum response. The decrease in maximum response is however accompanied by an increase in the range of rpms in which the amplitudes of the response is significant.

Cross-stiffness terms have a notable effect on the response of the non-accelerating rotor but not on the accelerating rotor unless the magnitude of the cross term is extremely high. The magnitudes at which there was found to be an effect in the model are probably unrealistically high for an actual cross term. The cross-stiffness terms have very little effect on the amplitude of the lateral bending response of an accelerating rotor.

The initial findings of acceleration scheduling are encouraging. Although the evaluation performed on the model was limited in its flexibility and optimization, it did disclose the possibility of reducing the maximum rotor response by taking advantage of the apparent shift in the critical speed. This may prove to be an extremely promising approach in which to reduce the lateral bending response.

In this analysis, the effects of each of the parameters were studied individually. No analysis was performed to determine which combinations of parameters would give the best response. Certainly, a combination of these beneficial factors can be applied to give the best overall reduction in the maximum lateral bending amplitude of a rotor transitioning through its critical speed.

VI. CONCLUSIONS AND RECOMMENDATIONS

A. SUMMARY AND CONCLUSIONS

An analytical model was developed to predict the response of a simple accelerating rotor and a parametric study was conducted to determine possible ways to minimize the magnitude of the response and/or reduce the number of cycles occurring at the higher magnitudes.

Significant reductions in the maximum response amplitude of a rotor transitioning through its critical speed are achievable. This is best accomplished by the following methods:

1. Decrease the forcing function by balancing the rotor.
2. If using a constant rate of acceleration, use as great as an acceleration rate as practical.
3. Increase damping.
4. Achieve stiffness symmetry if possible, but if not, use a great enough asymmetry to minimize the response.

Furthermore, the analytical model predicted that acceleration scheduling could reduce the magnitude and duration of the response.

Experimental data with varying rates of acceleration were compared to the model with very accurate results.

B. RECOMMENDATIONS

There are many ways in which the experimental facility could be further modified to allow a more wide variety of investigations into the rotordynamic field. In addition, there are many ways in which the facility can be further utilized in it's present configuration.

1. **Determine the exact time that each data acquisition occurs.**

As stated earlier, an attempt was made to allow for the exact time of, or time between acquisitions to be outputted in a matrix with the x and y displacement data. This is very important in that it would allow for phase locking the data and being able to determine the precise rate of acceleration and the rpm at which each acquisition occurred. This would give a much more precise picture of all aspects of the rotordynamic response. Continued attempts in this area are highly recommended.

2. **Increase the allowable acceleration rates in the rotor kit.**

The rotor kit is only capable of a maximum acceleration rate of 15000 rpm/min. This is still a relatively slow rate of acceleration and therefore gives a limited range in which to determine the effects of acceleration. Discussions with the Bentley Nevada Corporation revealed the prospect of changing the motor controller feedback circuit to increase these rates. The drive motor may then be capable of accelerations of 30,000 rpm/min or greater.

3. **Develop a way to vary the stiffness and damping on the rotor kit.**

The experimental facility has much less flexibility than the computer models in that you cannot vary the stiffness or damping. As discussed in Chapter IV, the mounting table had a great effect on these values. If the characteristics of the mounting table could be changed, by shorting the resilient mounts mechanically for instance, the effects of varying stiffness and damping could, at a minimum, be qualitatively observed.

4. **Conduct a more detailed analysis of acceleration scheduling.**

The results obtained by instantaneously changing the rate of acceleration discussed in Chapter III look promising. Further research in the area of optimizing an acceleration schedule through critical could prove beneficial. If analysis does show that acceleration

scheduling is a feasible means of reducing the maximum amplitude and/or the amount of time the rotor experiences significantly large vibrational amplitudes, then experiments should be performed to verify the analysis. This would require a different motor controller than is currently installed on the experimental facility. A computer controlled motor controller capable of scheduling the acceleration rate would be necessary.

APPENDIX. LIST OF DIMENSIONS AND PROPERTIES

Rotor Shaft:

Material:	4140 Low Alloy Steel	
Modulus of Elasticity:	200 GPa	29.2(10^6) psi
Length:	45.7 cm	18.0 in
Diameter	0.9525 cm	0.375 in
Mass	0.253 kg	0.558 lbm
Density	7766 kg/m^3	0.281 lbm/in^3

Rotor Disk:

Material:	316 Stainless Steel	
Width:	2.54 cm	1.0 in
Inner Diameter	0.9525 cm	0.375 in
Outer Diameter	1.18 cm	3.0 in
Mass	0.816 kg	1.8 lbm

LIST OF REFERENCES

1. Lewis, F. M., "Vibration During Acceleration Through a Critical Speed," Journal of Applied Mechanics, Trans. ASME, Vol.54, 1932.

2. Vejvoda, C. E., "Analytical and Experimental Investigation of Rotordynamic Response and Backward Whirl Induced by Split Resonance," Master's Thesis, Naval Postgraduate School, Monterey, California, December 1994.

3. Rankine, W.A., "On the Centrifugal Force of Rotating Shafts," *London Engineer*, v.27, p.249, 1869.

4. Jeffcott, H. H., "The Lateral Vibration of Loaded Shafts in the Neighborhood of a Whirling Speed - The Effect of Want of Balance," *London Philosophical Magazine,* v. 37, pp. 304-314, 1919.

5. Baker, J. G., "Mathematical-Machine Determination of the Vibration of Accelerated Unbalanced Rotor," Journal of Applied Mechanics, Trans. ASME, Vol. 6, 1939.

6. Meuser, R. B. and Weibel, E. E., "Vibration of a Nonlinear System During Acceleration Through Resonance," Journal of Applied Mechanics, Trans. ASME, Vol. 15, 1948.

7. McCann, Jr., G. D. and Bennett, R. R., "Vibrations of Multifrequency Systems During Acceleration Through Critical Speeds," Journal of Applied Mechanics, Trans. ASME, Vol. 16, 1949.

8. Fearn, R. L. and Millsaps, K., "Constant Acceleration of an Undamped Simple Vibrator Through Resonance," Journal of the Royal Aeronautical Society, p.567, August 1967.

9. Gluse, M. R., "Acceleration of an Unbalanced Rotor Through its Critical Speeds," Naval Engineers Journal, pp. 135-144, February 1967.

10. Ishida, Y., Yamamoto, T. and Murakami, S., "Nonstationary Vibration of a Rotating Shaft with Nonlinear Spring Characteristics During Acceleration Through a Critical Speed," JSME International Journal, Series III, Vol. 35, No. 3, 1992.

11. Vance, J.M., *Rotordynamics of Turbomachinery*, pp. 130-131, John Wiley & Sons, 1988.

12. Simei, F.A., "Development of an Experimental Facility for Analysis of Rotordynamic Phenomena," Master's Thesis, Naval Postgraduate School, Monterey, California, March 1994.

INITIAL DISTRIBUTION LIST

1. Defense Technical Information Center.....2
   8725 John J. Kingman Rd., STE 0944
   Ft. Belvoir, Virginia 22060-6218

2. Library, Code 13.....2
   Naval Postgraduate School
   Monterey, California 93943-5101

3. Department Chairman, Code ME.....1
   Department of Mechanical Engineering
   Naval Postgraduate School
   Monterey, California 93943-5000

4. Professor Knox T. Millsaps Jr., Code ME/MI.....4
   Department of Mechanical Engineering
   Naval Postgraduate School
   Monterey, California 93943-5000

5. LT. Gregory L. Reed.....2
   935 Grace Dr.
   Carmel, Indiana 46032

6. Curricular Officer, Code 34.....1
   Department of Mechanical Engineering
   Naval Postgraduate School
   Monterey, California 93943-5100

7. Mr. Dan Groghan.....1
   Director Engine Division, SEA-03X3
   NAVSEA HQ, NC4
   2341 Jefferson Davis Highway
   Arlington, VA 22242-5160

8. Mr. John Hartranf.....1
   Manager LM-2500, SEA-03X34
   NAVSEA HQ, NC4
   2341 Jefferson Davis Highway
   Arlington, VA 22242-5160

9. Professor R.L. Fearn.....1
   Department of Aerospace Engineering
   University of Florida @
   Gainesville, FL 32611

10. Dr. Brian Murphy.....1
Center for Electromechanics
Mail Stop R7000
University of Texas
Austin, TX 78712

11. Bentley Nevada Corporation.....1
Mr. Don Bentley
P.O. Box 157
Minden, Nevada 89423

12. Dr. John Vance.....1
Department of Mechanical Engineering
Texas A & M University
College Station, Texas 77843-3123

13. Mr. Doug Lake.....1
Office of Naval Research
800 N. Quincy St.
Arlington, VA 22217-5660